Article

Cell Reports

PCNA Deubiquitylases Control DNA Damage Bypass at Replication Forks

Graphical Abstract

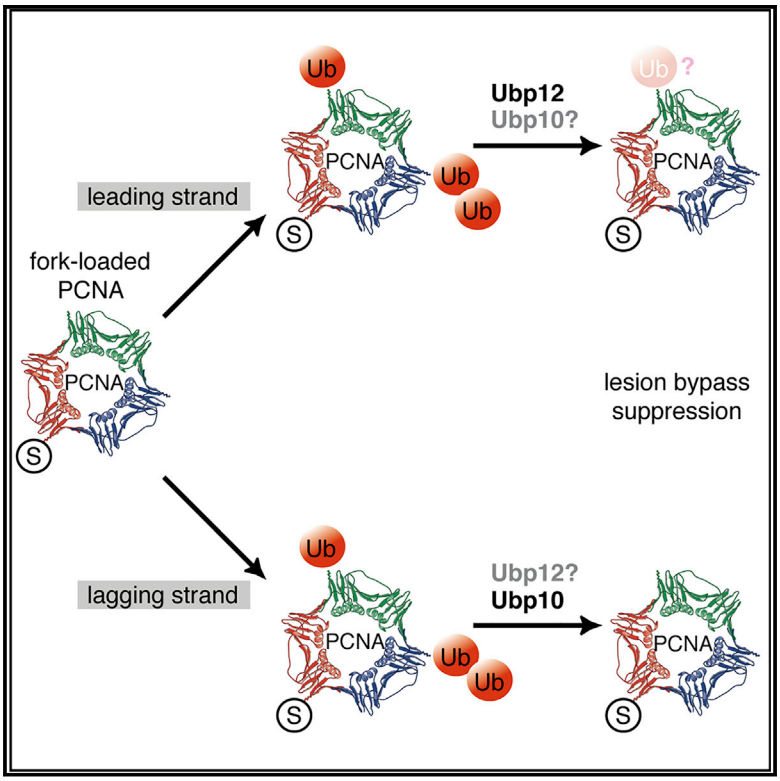

Authors

Vanesa Álvarez, Camilla Frattini, María P. Sacristán, Alfonso Gallego-Sánchez, Rodrigo Bermejo, Avelino Bueno

Correspondence

rodrigo.bermejo@csic.es (R.B.), abn@usal.es (A.B.)

In Brief

Álvarez et al. reveal a mechanism that modulates DNA damage tolerance to promote processive DNA synthesis. Ubp10 and Ubp12 ubiquitin proteases bind replication forks and distinctly cooperate to revert the ubiquitylation of the essential replication factor PCNA at lysine 164, hence restraining DNA damage tolerance events engaging nascent strands.

Highlights

- Ubp10 and Ubp12 DUBs remove ubiquitin from PCNA^{K164} with distinct chain preferences
- Fork association of Ubp10, but not Ubp12, depends on PCNA binding to lagging strands
- PCNA-DUBs counteract template switch and Rev1 TLS factor binding to replication forks
- Ubp10- and Ubp12-mediated PCNA^{K164} deubiquitylation promotes processive DNA replication

Álvarez et al., 2019, Cell Reports *29*, 1323–1335
October 29, 2019
https://doi.org/10.1016/j.celrep.2019.09.054

CellPress

Cell Reports
Article

PCNA Deubiquitylases Control DNA Damage Bypass at Replication Forks

Vanesa Álvarez,[1,4] Camilla Frattini,[2,4] María P. Sacristán,[1,3,4] Alfonso Gallego-Sánchez,[1] Rodrigo Bermejo,[2,*] and Avelino Bueno[1,3,5,*]
[1]Instituto de Biología Molecular y Celular del Cáncer (USAL/CSIC), Salamanca, Spain
[2]Centro de Investigaciones Biológicas (CSIC), Madrid, Spain
[3]Departamento de Microbiología y Genética, Universidad de Salamanca, Salamanca, Spain
[4]These authors contributed equally
[5]Lead Contact
*Correspondence: rodrigo.bermejo@csic.es (R.B.), abn@usal.es (A.B.)
https://doi.org/10.1016/j.celrep.2019.09.054

SUMMARY

DNA damage tolerance plays a key role in protecting cell viability through translesion synthesis and template switching-mediated bypass of genotoxic polymerase-blocking base lesions. Both tolerance pathways critically rely on ubiquitylation of the proliferating-cell nuclear antigen (PCNA) on lysine 164 and have been proposed to operate uncoupled from replication. We report that Ubp10 and Ubp12 ubiquitin proteases differentially cooperate in PCNA deubiquitylation, owing to distinct activities on PCNA-linked ubiquitin chains. Ubp10 and Ubp12 associate with replication forks in a fashion determined by Ubp10 dependency on lagging-strand PCNA residence, and they downregulate translesion polymerase recruitment and template switch events engaging nascent strands. These findings reveal PCNA^{K164} deubiquitylation as a key mechanism for the modulation of lesion bypass during replication, which might set a framework for establishing strand-differential pathway choices. We propose that damage tolerance is tempered at replication forks to limit the extension of bypass events and sustain chromosome replication rates.

INTRODUCTION

Cells are exposed to the challenge of endogenous and exogenous DNA damage, a major source of genomic instability and, in multicellular organisms, a driving force for cancer. Cells are particularly sensitive to DNA damage occurring during replication due to the stringent nature of replicative DNA polymerases, which fail to accommodate damaged bases and can get blocked, with harmful effects for cell viability and genome integrity. To cope with base damage during DNA replication, cells have evolved damage-tolerance mechanisms that allow circumventing DNA lesions and allegedly ensure a timely coordination between the progression of replication forks and DNA repair (Chang and Cimprich, 2009; Friedberg, 2005; Lawrence, 1994).

DNA damage tolerance (DDT) is exerted through two major pathways: translesion synthesis (TLS) and template switching (TS), which employ different mechanisms to overcome the potentially lethal effects of the engagement by replication machineries of lesions impeding the progression of replicative DNA polymerases (Friedberg, 2005). Though DDT has been referred to as post-replication repair, it is currently accepted that it is more than a repair mechanism per se, as it allows circumventing DNA lesions, either by the use of specialized polymerases or by employing newly synthesized sister chromatids as damage-free templates (Chang and Cimprich, 2009; Garg and Burgers, 2005; Ghosal and Chen, 2013; Ulrich, 2006). Indeed, the identification of specialized, evolutionary conserved, alternative DNA polymerases with the ability to replicate across damaged bases and effectively bypass lesions was a landmark discovery, revealing the existence of mechanisms to tolerate DNA damage during replication (Friedberg and Gerlach, 1999). These enzymes, known as TLS DNA polymerases, are error prone and potentially mutagenic, as their ability to accommodate templates with bulky lesions contributes to a low fidelity, and they lack intrinsic proofreading activities. Conversely, TS-based DDT mechanisms are, in principle, error-free, as they are thought to involve the pairing of a blocked nascent strand with its sister in order to copy an intact base. TS plays an important but not yet fully understood role during chromosome replication, evolutionarily conserved throughout eukaryotes (reviewed by Branzei, 2011).

The proliferative cell nuclear antigen (PCNA) replicative polymerase processivity factor is a key mediator of DDT in eukaryotes (Bergink and Jentsch, 2009; Hoege et al., 2002; Ulrich, 2009). Monoubiquitylation of PCNA on Lys164 (ubPCNA^{K164}) promotes DNA polymerase-mediated error-prone TLS. Instead, the addition of Lys^{63}-linked ubiquitin moieties to mono-ubPCNA^{K164} promotes an error-free mechanism based on TS (Branzei and Foiani, 2010; Kannouche et al., 2004; Stelter and Ulrich, 2003; Ulrich, 2009; Vanoli et al., 2010; Watanabe et al., 2004; Zhang and Lawrence, 2005). PCNA^{K164} monoubiquitylation is catalyzed by the Rad6/Rad18 (E2/E3) ubiquitin ligase (Hedglin and Benkovic, 2015; Hoege et al., 2002; Stelter and Ulrich, 2003), while PCNA^{K164} polyubiquitylation depends on a PCNA-ubiquitin ligase complex conformed by Rad5, Mms2, and Ubc13 (Lawrence, 1994; Zhang and Lawrence, 2005). As PCNA polyubiquitylation relies on the previous monoubiquitylation of PCNA on K164,

Rad6/Rad18 function is essential for both TLS and TS DDT pathways (Hedglin and Benkovic, 2015). Rad6 group proteins are conserved from unicellular eukaryotes to mammals and, in all models tested to date, Rad6/Rad18 monoubiquitylates PCNA^{K164} in response to replication stress and a variety of DNA damaging agents, highlighting the significance of this pathway (Arakawa et al., 2006; Frampton et al., 2006; Hoege et al., 2002; Kannouche et al., 2004; Watanabe et al., 2004). It is therefore broadly considered that PCNA^{K164} is ubiquitylated in response to DNA damage. In line with this view, PCNA monoubiquitylation is not observed during unchallenged replication in most organisms (Daigaku et al., 2010; Davies et al., 2008; Hoege et al., 2002; Karras and Jentsch, 2010), with the exception of fission yeast and *Xenopus* eggs, in which the role played by this modification in S phase remains obscure (Álvarez et al., 2016; Daigaku et al., 2017; Frampton et al., 2006; Leach and Michael, 2005).

The Rad6/Rad18 complex is recruited to replication forks upon replication protein A (RPA) accumulation downstream of DNA lesions during the initial steps of the cellular response to DNA damage (Chang et al., 2006; Davies et al., 2008; Haracska et al., 2006; Hedglin and Benkovic, 2015; Hoege et al., 2002; Niimi et al., 2008). However, the spatiotemporal context in which Rad6/18-mediated PCNA^{K163} ubiquitylation triggers DDT mechanisms is still under debate, as Rad18 has also been identified at nascent DNA in unperturbed cells (Alabert et al., 2014; Dungrawala et al., 2015; Kile et al., 2015). Despite conflicting evidence, it was initially suggested that DTT occurs during the S phase to facilitate the completion of chromosome replication (Daigaku et al., 2010; Ulrich, 2011). However, it was later shown that Rad18-dependent PCNA ubiquitylation can operate after bulk genome replication (Daigaku et al., 2010; Karras and Jentsch, 2010), supporting the notion that DDT may work as a post-replicative mechanism (Karras and Jentsch, 2010). It is generally accepted that TLS may operate on the fly to prevent replication fork blockage, though direct evidence for this fact is missing to date. This, however, might not be a preferred option, as the low fidelity of TLS polymerases increases the risk of introducing mutations opposite to DNA lesions (Hoege et al., 2002; Stelter and Ulrich, 2003). Lesion bypass through TS is error free, but it involves certain risks for cells due to the formation of structures linking sister chromatids that must be effectively resolved to achieve chromosome segregation (Branzei, 2011; see also references therein). Hence, mechanisms limiting lesion bypass events at nascent DNA might be required to minimize deleterious side effects associated with the TLS and TS pathways' usage.

Ubiquitin moieties conjugated to PCNA-K164 can be removed by specialized ubiquitin proteases (or PCNA^{K164}-deubiquitylating enzymes [DUBs]). Mammalian Usp1, Usp7, and Usp10 and budding yeast Ubp10 revert PCNA ubiquitylation occurring in response to exogenous DNA damage (Gallego-Sánchez et al., 2012; Huang et al., 2006; Mailand et al., 2013; Park et al., 2014). Additionally, the Ubp10-ortholog Ubp16 cooperates with the Ubp2, Ubp12, and Ubp15 ubiquitin proteases to revert PCNA^{K164} ubiquitylation in the fission yeast *Schizosaccharomyces pombe* (Álvarez et al., 2016). Based on indirect evidence, PCNA^{K164}-DUBs have been proposed to suppress DDT events (Gallego-Sánchez et al., 2012; Huang et al., 2006; Mailand et al., 2013; Park et al., 2014). However, the mechanistic involvement of PCNA deubiquitylation in controlling both DDT pathways and the timing of PCNA^{K164}-DUBs action during the replication of damaged DNA templates remains unknown.

Here, we show that in budding yeast cells, the Ubp10 and Ubp12 PCNA^{K164}-DUBs physically interact with the PCNA and cooperate in its deubiquitylation, exhibiting a differential preference in the removal of K164-linked ubiquitin chains. While addressing the spatiotemporal framework of PCNA deubiquitylation, we found that both Ubp10 and Ubp12 associate with replication forks, the former in a fashion influenced by PCNA unloading from lagging strands. Furthermore, inactivation of Ubp10 and Ubp12 exacerbates both TS events and the recruitment of TLS polymerase ζ-associated protein Rev1 to stalled replication forks, which hints at a complex regulation of lesion bypass pathways. Our data reveal that the reversion of PCNA^{K164}-ubiquitylation is a key mechanism modulating DDT during DNA synthesis, which we propose might limit the extension of bypass events and support normal replication rates during unperturbed replication.

RESULTS

Ubp10 and Ubp12 Proteases Diversely Cooperate to Deubiquitylate PCNA in the S Phase

The Ubp10 ubiquitin protease reverts PCNA ubiquitylation in *Saccharomyces cerevisiae* (Gallego-Sánchez et al., 2012). However, Ubp10 ablation does not result in the accumulation of Ub-PCNA in unperturbed cells, pointing at the involvement of additional enzymes in PCNA deubiquitylation during replication in this organism (Gallego-Sánchez et al., 2012). To identify additional PCNA-DUBs, we screened cells lacking individual ubiquitin proteases in combination with *UBP10* deletion for an accumulation of Ub-PCNA (unpublished data). Using this approach, we found that a combined ablation of Ubp10 and Ubp12 resulted in the accumulation of both mono- (Ub) and di-ubiquitylated (Ub_2) PCNA in asynchronously cycling cells (Figure 1A; Asyn), with equivalent sumoylated (SUMO) PCNA levels. Elimination of Ubp12 alone did not result in a robust accumulation of ubiquitylated PCNA in unperturbed cycling cells—similar to what was observed for *UBP10* deletion—or upon the induction of replication stress by treatment with the alkylating agent methyl methanesulphonate (MMS) or the ribonucleotide reductase inhibitor hydroxyurea (HU) (Figure 1B; compare lanes 1 and 3). In contrast, a combination of *ubp10*Δ and *ubp12*Δ determined a marked synergistic increase in ubiquitylated PCNA levels in both cycling and HU/MMS-treated cells (Figure 1B; compare lanes 1 and 4), which did not take place in G1-arrested cells (Figure 1A), suggesting that Ubp10 and Ubp12 cooperate to achieve PCNA deubiquitylation in the S phase.

We next directly analyzed the *in vivo* and *in vitro* abilities of Ubp12 to counteract PCNA ubiquitylation owing to MMS-induced S-phase damage. In keeping with previous observations (Gallego-Sánchez et al., 2012), overexpression of *UBP10* counteracted the accumulation of both Ub- and Ub_2-PCNA (absent in cells ablated for the Rad18 E3 ligase) (Figure 1C). In

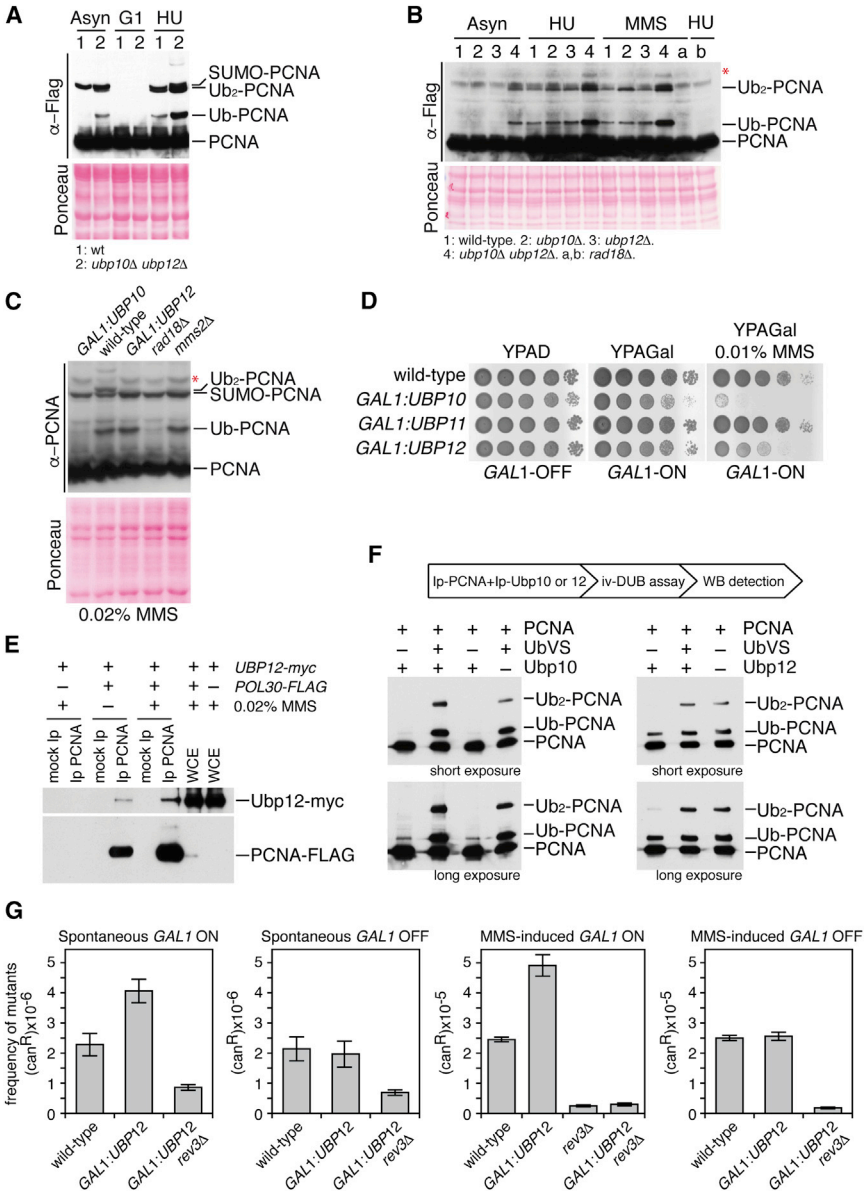

Figure 1. Ubp10 and Ubp12 Ubiquitin Proteases Cooperate to Revert PCNA Ubiquitylation

(A and B) Accumulation of ubiquitylated PCNA in exponentially growing (Asyn), α-factor blocked (G1), MMS- or HU-treated wild-type, *ubp10Δ*, *ubp12Δ*, and *ubp10Δ ubp12Δ* cells. MMS- or HU-treated *rad18Δ* controls are shown (lanes A and B, respectively). Cell extracts were resolved in 12% polyacrylamide SDS gels and immunoblotted with α-FLAG antibodies. Ponceau stainings are shown as additional loading controls.

(C) Immunodetection of ubiquitylated and di-ubiquitylated PCNA forms in wild-type cells, in cells induced (*GAL1:UBP*) for Ubp10 or Ubp12 expression and in controls, after a 90-min treatment with 0.02% MMS. Trichloroacetic acid (TCA) extracts were processed for immunoblotting with affinity purified rabbit α-PCNA antibodies.

(D) Ten-fold dilutions of *GAL1*-driven *UBP10*-, *UBP11*- (negative control), and *UBP12*-overexpressing cells incubated at 25°C in glucose or galactose plates in the absence or the presence of 0.01% MMS for 60 h.

(E) Co-immunoprecipitation assay of Ubp12-myc and FLAG-tagged PCNA. PCNA-FLAG was immunoprecipitated from both untreated cells or after 90 min of treatment with 0.02% MMS (as indicated). Blots were incubated with α-myc or α-FLAG antibodies. Whole-cell extracts (WCEs) are shown for reference. Strains used in the assays are indicated.

(F) PCNA *in vitro* deubiquitylation assay. Mono- and di-ubiquitylated PCNA was obtained by immunoprecipitation with anti-FLAG antibodies from *ubp12*, *ubp15*, and *ubp16 pcn1*-FLAG *S. pombe* cells. PCNA samples were split and incubated with immunoprecipitated Ubp10-myc or Ubp12-myc in the absence or in the presence of UbVS to inhibit ubiquitin-processing protease (UBP) activity (see STAR Methods for details). An untreated aliquot serves as a reference for immunoprecipitated PCNA. PCNA ubiquitylation state was inferred by the distinctive mobility on SDS-PAGE gels of PCNA forms.

(G) Forward mutation analysis in *GAL1:UBP12* strains. Canavanine resistance was assayed in wild-type, *GAL1:UBP12*, *rev3Δ*, and *GAL1:UBP12 rev3Δ* cells incubated in either galactose (GAL ON) or glucose to induce or repress *UBP12* expression, respectively, and treated or not with 0.005% MMS (spontaneous and MMS induced, as indicated). Means and SDs of three independent experiments are shown.

contrast, *UBP12* overexpression preferentially downregulated Ub_2-PCNA forms (not present in *mms2* mutants) (Figure 1C). Consistent with a putative failure to effectively activate DDT pathways owing to suppressed PCNA ubiquitylation, overexpression of Ubp12 conferred sensitivity to MMS-induced damage similarly, though to a lesser extent, as to that observed for Ubp10 (Figure 1D). We addressed the physical interaction between Ubp12 and PCNA by testing PCNA immunoprecipitates for the presence of myc-epitope tagged Ubp12 and found that Ubp12 interacts *in vivo* with the sliding clamp in both unperturbed and MMS-treated cells (Figure 1E), similarly to what was previously described for Ubp10 (Gallego-Sánchez et al., 2012). The intensity of Ubp12-PCNA interaction, nonetheless, lessened as cells progressed through S phase in the presence of the alkylating chemical (Figures S1A and S1B), likely as a consequence of a progressive decline in the number of stalled replication forks (Jossen and Bermejo, 2013; Tercero and Diffley, 2001).

We next performed *in vitro* ubiquitin protease assays to examine the activity of Ubp10 and Ubp12 on ubiquitylated PCNA. As a source of Ub- and Ub_2-PCNA, we immunoprecipitated it from *S. pombe ubp12 ubp15 ubp16 pcn1*-FLAG-epitope tag (FLAG) cell extracts (Álvarez et al., 2016), as fission yeast cells do not SUMOylate the sliding clamp (Álvarez et al., 2016; Daigaku et al., 2017; Frampton et al., 2006). Ubp10-myc efficiently deubiquitylated both Ub- and Ub_2-PCNA in a fashion

blocked by the ubiquitin vinyl sulfone (UbVS) irreversible DUB inhibitor (Figure 1F) and dependent on its catalytic activity (Figure S1C). In contrast, Ubp12-myc removed Ub_2-PCNA forms only, showing poor activity on Ub-PCNA in the same conditions (Figures 1F and S1C). This differential *in vitro* activity is unlikely to be caused by a defective interaction of Ubp12 with Schizosaccharomyces pombe PCNA (SpPCNA), as Ubp12 can effectively remove Ub_2-SpPCNA and is consistent with the *in vivo* effects observed upon DUBs overexpression. In concordance with the reduction in poly-Ub PCNA levels, we found that *UBP12* overexpression causes a dosage mutator phenotype that depends on Rev3 (Figure 1G) and is hypostatic to that of *mms2* deletion (Figure S1D) (Ang et al., 2016), likely caused by an abrogation of TS events driving tolerance through TLS. This *in vivo* and *in vitro* evidence reveals a differential preference of these enzymes during PCNA deubiquitylation, as Ubp10 may efficiently remove all ubiquitins linked to $PCNA^{K164}$ (single ubiquitin monomers or K63-linked poly-ubiquitin chains), whereas Ubp12 may preferentially deconjugate K63-linked ubiquitin moieties from poly-ubiquitylated PCNA. Such differential abilities of PCNA-DUBs to render either Ub- or Ub_2-PCNA establishes a potential to diversely influence DDT pathways.

Association of Ubp10 and Ubp12 with Replication Forks Is Differentially Influenced by PCNA Association to Nascent Strands

The functional significance of PCNA deubiquitylation remains unclear to date. The reversion of Rad18-mediated ubiquitylation may represent a mean to locally influence the activity of DDT pathways. In order to address this issue, we investigated Ubp10 and Ubp12 localization genome-wide through chromatin immunoprecipitation (ChIP), followed by hybridization of microarrays (ChIP-on-chip) (Katou et al., 2003). We mapped the association of PCNA-DUBs with chromosomal DNA in cells released from a G1 arrest and synchronously replicating in the presence of 0.2 M HU. Under these conditions, replication forks emanating from early origins slow down and progress for about 5 kb (Bermejo et al., 2007; Shirahige et al., 1998). Approximate positions of replication forks along the genome were determined by analysis of the Mec1 checkpoint kinase co-factor Ddc2 (Figure 2A), which associates with single-stranded DNA (ssDNA) generated upon fork stalling (Lucca et al., 2004; Zou and Elledge, 2003). Ubp12 binding peaked, among other genomic loci, around the active early replication origins in the environment of stalled forks, as determined by Ddc2 signals. In contrast, an equivalent localization of Ubp10 at the replication forks was not detected in HU-arrested cells. We detected additional Ubp12 and Ubp10 signals in association with different genomic features (including telomeres, rDNA, and mating-type loci) unrelated to the stalled forks. These might reflect functions of these DUBs mediated by deubiquitylation of targets presumably different from PCNA, as in the case of the Ubp10 function in loci silencing (Emre et al., 2005; Gardner et al., 2005; Schulze et al., 2011).

We reasoned that a lack of Ubp10 association with replication forks could be a consequence of PCNA unloading from stalled lagging strands. When replication forks stall owing to reduced deoxynucleotide triphosphates (dNTPs) levels, an Elg1 alternative replication factor C (RFC) complex removes PCNA molecules from lagging strands (Ben-Aroya et al., 2003; Kubota et al., 2015, 2013). Thus, *elg1* deletion provides a genetic tool for strand-specific genomic analysis of proteins that interact with PCNA (Kubota et al., 2015; Yu et al., 2014). Indeed, when we compared Ubp10 localization in HU-arrested S-phase cells, additional enrichment clusters correlating with Ddc2 signals at replication forks became evident in *elg1*Δ mutants (Figures 2B and S2A), suggesting that the retention of lagging-strand PCNA determines Ubp10 binding to stalled replication forks. This association, quantitatively measured by ChIP-qPCR close to the *ARS305* replication origin, increased roughly 10-fold upon Elg1 ablation (Figure 2C), rendering an enrichment higher than that observed for Ubp12 in *ELG1* cells. In contrast, ablation of Elg1 did not influence the Ubp12 association with replication forks (Figures 2C and S2B), suggesting that this DUB does not bind lagging-strand PCNA. A transient enrichment of both Ubp10 and Ubp12 close to *ARS305* with timings consistent with fork passage was observed in the unperturbed S phase (Figure 2D), indicating that Ubp10 is present at forks when the lagging-strand PCNA is not unloaded. We note that Ubp12 and Ubp10 chromosome binding signals, similarly to Ddc2 binding, were not observed near late-firing or dormant origins inactive in HU-treated cells, indicating that origin-proximal DUB binding corresponds to sites of active replication only (Raghuraman et al., 2001; Santocanale and Diffley, 1998; Shirahige et al., 1998; Wyrick et al., 2001). In agreement with this notion, robust Ubp10 and Ubp12 active origin-related signals were not detected in G1- or G2-arrested cells (Figures 2D and S2C).

PCNA Deubiquitylation Counteracts Nascent Strand Engagement in TS Intermediates

We next examined the impact of PCNA deubiquitylation on the DDT at replication forks. We analyzed first the error-free DDT branch by visualizing TS intermediates through neutral/neutral 2D-gel electrophoresis (2D gels) in wild-type cells and *ubp10 ubp12* mutants replicating in the presence of MMS. TS drives the error-free branch of DNA damage bypass via a Rad51-/Rad52-mediated strand invasion mechanism that results in intermediates migrating in 2D gels as fully replicated X-shaped molecules (González-Prieto et al., 2013; Liberi et al., 2005; Mankouri and Hickson, 2006; Sollier et al., 2009; Vanoli et al., 2010), which link nascent sister chromatids before being dissolved by the Sgs1-Top3-Rmi1 complex (Bernstein et al., 2009; Giannattasio et al., 2014; Lopes et al., 2003). Single and double PCNA-DUB *ubp10 ubp12* mutants showed increased X-shaped intermediate levels during the replication of damaged chromosomal templates in a *SGS1* dissolution-proficient background (Figure 3A), indicating that PCNA deubiquitylation counteracts TS events. Accumulation of these molecules was transient, though they were still visible at later time points, particularly in mutants lacking Ubp10 that exhibit a delayed replication progression in the presence of MMS (Figure S3A), suggesting that either formation of these intermediates was promoted, or their resolution counteracted upon the impairment of PCNA-DUBs. Of note, the detection of X-shaped molecules

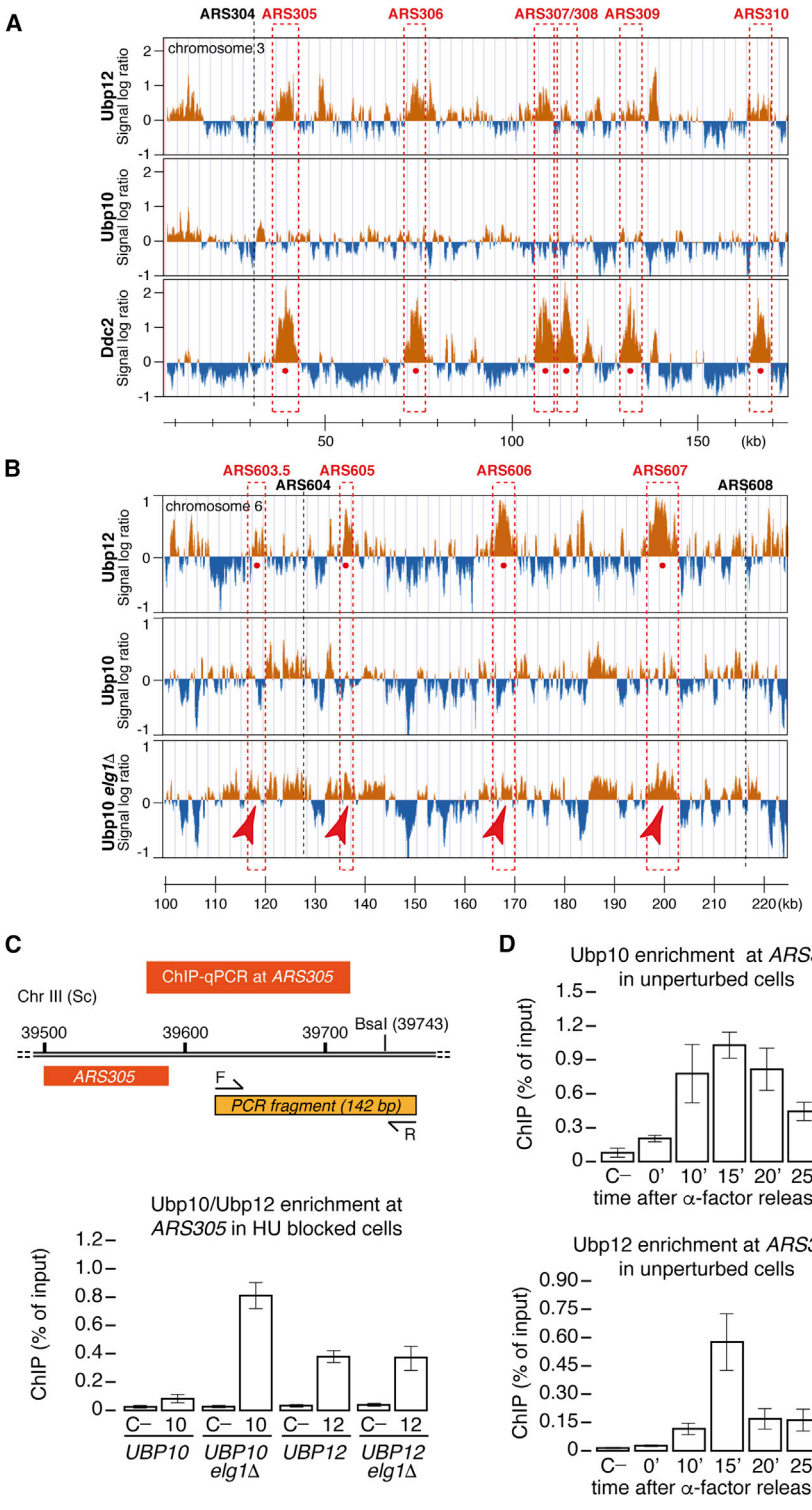

Figure 2. Ubp10 and Ubp12 PCNA-DUBs Associate with Replication Forks

(A) *UBP10-myc*-, *UBP12-myc*-, *DDC2-myc*-, and *elg1Δ UBP10-myc*-tagged cells were synchronized with α-factor and released for 1 h in 0.2 M HU. Samples were processed for ChIP with α-myc monoclonal antibodies. Orange histogram bars on the y axis show the average signal ratio of loci significantly enriched in the immunoprecipitated fraction in $\log_2$ scale. The x axis shows coordinates along chromosome III in kilobases. Early-firing (in red) and late/dormant (in black) replication origins are evidenced. The relative positions of early-firing origins and the extent of fork progression are indicated by red dots and dotted squares, respectively.

(B) ChIP analysis along chromosome VI performed as in (A), including *UBP10-myc elg1Δ* cells. Additional Ubp10 clusters localized around early-firing replication origins are indicated by red arrowheads.

(C) The indicated cells were cultured as in (A) and processed for ChIP-qPCR. Means and standard deviations of three independent experiments are shown. A schematic of the *ARS305*-proximal DNA fragment amplified is provided.

(D) Ubp10 and Ubp12 ChIP was performed at the indicated time points after release from an α-factor block in unperturbed conditions.

Means and SDs of three independent experiments are shown. “C−” denotes untagged controls.

in *ubp10* and *ubp12* mutants was abolished by ablation of Rad52, and their accumulation was precluded by expression of non-ubiquitylatable PCNA (in *pol30*^{K164R} cells) (Figures 3B, S3B, and S3C), indicating that a vast majority of Ubp10/12 ablation-related intermediates detected in 2D gels reflect bona fide TS events.

We performed similar experiments upon elimination of Sgs1 to monitor TS intermediate levels in a dissolution-defective background. Ablation of *ubp10* or *ubp12* largely anticipated the accumulation of TS intermediates (Figures 3C and S3D), supporting the notion that defective PCNA deubiquitylation due to DUB ablation promotes the engagement of daughter strands to form these molecules. Strikingly, analysis of replication intermediates upon HU-induced fork stalling revealed the accumulation of small Y-shaped intermediates in *ubp10* and, to a higher proportion, *ubp10 ubp12* mutants (Figure 4A), which differ from the canonical bubble and large Y molecules resulting from origin firing and fork progression (Figure 4B). Of note, accumulation of non-canonical small Ys was mirrored by a decrease in large Ys and, to a lesser extent, in bubble signals, suggesting that these molecules arise from transitions in which nascent DNA strands rearrange to alter the normal branched structure of replication intermediates. Accumulation of these small Y-shaped molecules was abolished by the ablation of

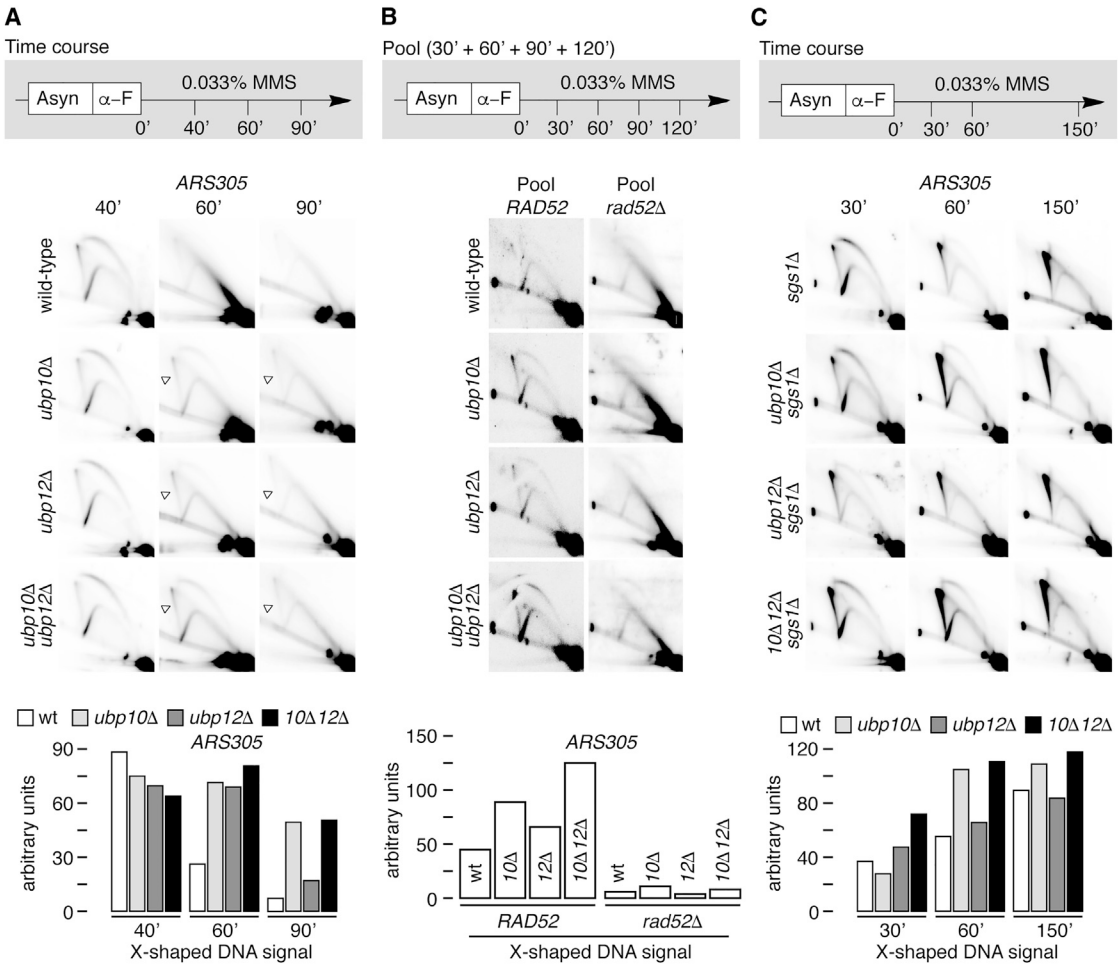

Figure 3. PCNA-DUBs Mutants Accumulate X-Shaped TS Intermediates

(A) Wild-type, *ubp10Δ*, *ubp12Δ*, and *ubp10Δ ubp12Δ* cells were synchronized with α-factor and released in the presence of 0.033% MMS. Samples were taken at the indicated times and processed for FACS analysis of DNA content (Figure S3A) and 2D-gel analysis of replication intermediates. Genomic DNA was cut with NcoI, electrophoresed in N:N 2D gels, transferred to nylon membranes, and hybridized to a probe spanning the *ARS305* early origin of replication. Quantification of the relative abundance of X-shaped DNA signals (indicated by open triangles) is shown.

(B) Wild-type, *ubp10Δ*, *ubp12Δ*, and *ubp10Δ ubp12Δ* cells in a *RAD52* wild-type or *rad52Δ* mutant background were treated as in (A). Samples were taken at the indicated times and pooled before preparation for 2D-gel analysis as in (A). Histogram plots show the quantification of the X-shaped DNA signals. FACS analysis is shown in Figure S3B.

(C) *sgs1Δ*, *sgs1Δ ubp10Δ*, *sgs1Δ ubp12Δ*, and *sgs1Δ ubp10Δ ubp12Δ* cells were treated as in (A). Samples were taken at the indicated intervals and processed for analysis of DNA content by FACS (shown in Figure S3C) and 2D-gel analysis as in (A). Histogram plots of the X-shaped DNA signals are shown.

All experiments in the figure were replicated two times.

Rad52 (Figure 4A), indicating that they likely result from TS events, described to be triggered upon polymerase stalling owing to dNTP shortage (Gallo et al., 2019). Taken together, these observations reveal the existence of a PCNA-DUB-driven mechanism counteracting the engagement of nascent DNA strands in TS events upon replication fork stalling by template lesions or dNTP shortage.

PCNA-DUBs Restrain TLS Polymerase ζ Complex Recruitment to Replication Forks

We next analyzed whether PCNA deubiquitylation influences the error-prone branch of the DDT pathway as well. For this, we studied the chromosomal localization of TLS polymerase ζ-associated Rev1 protein by ChIP-on-chip in cells released from a G1 arrest into a synchronous S phase in the presence of HU. We failed to observe Rev1 recruitment to replication forks in wild-type or PCNA-DUB-proficient cells or *ubp10 ubp12* double mutants (Figure S4A), suggesting that if Polymerase ζ is recruited to stalled forks in these conditions, its binding might be too weak or transient to be detected by ChIP. We also analyzed the impact of combined defects in PCNA deubiquitylation and Elg1-mediated unloading on Rev1 chromosomal binding (see strategy in Figure 5A). Strikingly, while Elg1 ablation alone bore no effect, its combination with the deletion of *ubp10* and *ubp12* resulted in the detection of sharp origin-proximal Rev1 signals (Figures 5B and S4A)—tightly matching

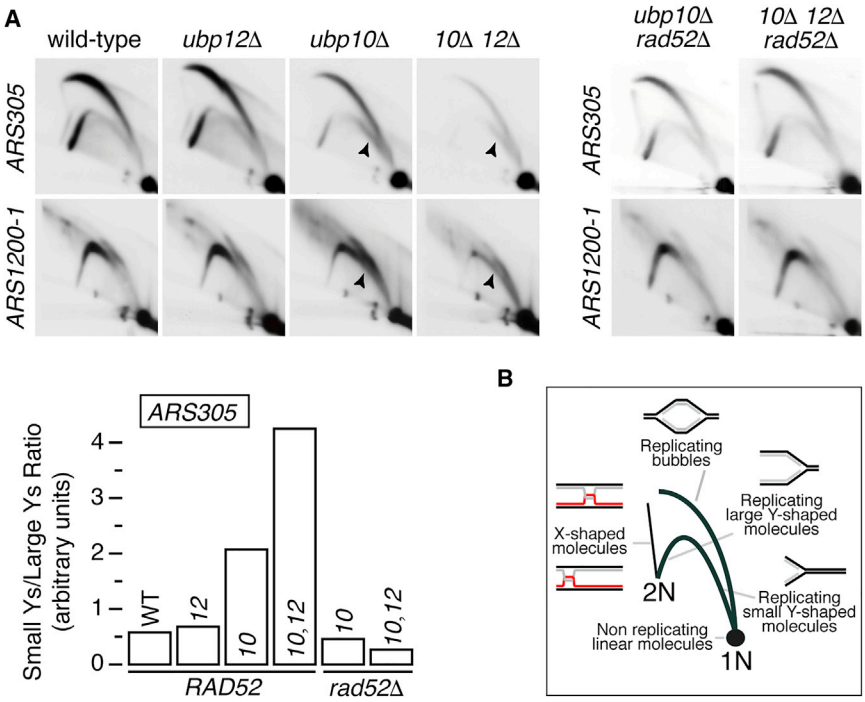

Figure 4. Accumulation of Putative Rad52-Dependent TS Intermediates at Stalled Forks in *ubp10Δ ubp12Δ* Mutants

(A) Wild-type, *ubp10Δ*, *ubp12Δ*, *ubp10Δ ubp12Δ*, *ubp10Δ rad52Δ*, and *ubp10Δ ubp12Δ rad52Δ* cells were synchronized with α-factor and released in the presence of 0.2 M HU. Samples were taken after 60 min and processed for 2D-gel analysis. Membranes were consecutively hybridized to probes spanning *ARS305* and *ARS1200-1* replication origins. Histogram plots of small/large Y-shaped intermediate ratios in *RAD52* and *rad52Δ* backgrounds of wild-type, *ubp10*, *ubp12*, and *ubp10 ubp12* DUB mutants are shown.

(B) Schematic of canonical replication intermediates and fully replicated joint molecules detected by 2D-gel analysis. Canonical small Ys reflect passive replication by forks emanating outside the probed fragment.

All experiments in the figure were replicated three times.

the positions of stalled forks, evidenced by Ddc2 binding—along entire chromosomes (Figure S4B). These results indicate that Rev1 association with stalled replication forks is counteracted by both PCNA deubiquitylases and PCNA unloading from lagging strands. Rev1 association to forks was not affected by the ablation of Mms2, required for PCNA di/poly-ubiquitylation (Figure S4C), consistent with its recruitment being promoted by PCNA mono-ubiquitylation only. Quantitative analysis close to the *ARS305* origin by ChIP-qPCR failed to detect robust Rev1 enrichment in *ubp10*Δ *elg1*Δ or *ubp12*Δ *elg1*Δ cells (Figure 5C), suggesting that the action of either DUB is sufficient to counteract Rev1 binding to forks. These data suggest that DNA polymerase ζ might be electively recruited to replication forks in an attempt to bypass replication blocks on the fly. In addition, they suggest that error-prone TLS lesion bypass events at forks are suppressed through a dual mechanism, requiring both PCNA deubiquitylation and removal from lagging strands.

PCNA Deubiquitylation Promotes Processive Replication by Suppressing TLS Events

Our findings point at the use of TS and TLS damage-tolerance pathways being controlled by Ubp10 and Ubp12 PCNA-DUBs at replication forks. In addition, the slow completion of bulk genome replication in *ubp10* MMS-treated cells (Figure S3) signified a key role for this PCNA-DUB in promoting replication in the presence of alkylating damage. Hence, we examined the biological significance of PCNA deubiquitylation-mediated DDT suppression in supporting the progression of chromosome replication. Replication defects in *ubp10Δ* cells most likely result from an excessive PCNA ubiquitylation, as they are suppressed by mutation of lysine 164 of PCNA to a non-ubiquitylatable arginine residue (Figure S5), which abrogates both the error-prone and error-free DDT pathways (Hoege et al., 2002; Stelter and Ulrich, 2003). Of note, cells ablated for Ubp10 also exhibit delayed bulk genome replication and S-phase completion in the absence of genotoxic insults (Figure S6), arguing for a fundamental requirement of PCNA deubiquitylation in sustaining normal chromosome replication rates.

One possibility is that PCNA-DUBs are constitutively recruited to replication forks to limit engagement in DDT processes and support steady replication progression. We tested this hypothesis by monitoring bulk replication progression in wild-type cells, *ubp10Δ* mutants, and cells in which *ubp10* deletion was combined with TLS Polymerase ζ and Pol η ablation by deletion of *REV1 REV3* and *RAD30* genes (*ubp10Δ tlsΔ*). Cells were released from G1 into S phase, and bulk genome replication was followed by fluorescence-activated cell sorting (FACS) in the absence or presence of MMS (Figures 6A and 6B). In both conditions, ablation of TLS DNA polymerases alleviated the replication progression defect of *ubp10Δ* cells. These observations suggest that the Ubp10 PCNA-K164 deubiquitylation-dependent role in supporting normal replication rates is linked to the function of, at least, the TLS branch of DDT. Taken together with our previous observation that PCNA-deubiquitylation counteracts Polymerase ζ association to replication forks, this evidence also indicates that PCNA-DUBs might help sustain replication rates by limiting exchanges between replicative and TLS DNA-polymerases. Based on these findings, we propose that fork-coupled DUBs act to constitutively promote PCNA deubiquitylation in order to limit excessive engagement of DDT processes and ensure processive chromosome replication.

DISCUSSION

Here, we studied the spatiotemporal determinants and functional impact of PCNA deubiquitylation as a mean to control DDT in budding yeast. We identified Ubp12 as a player acting

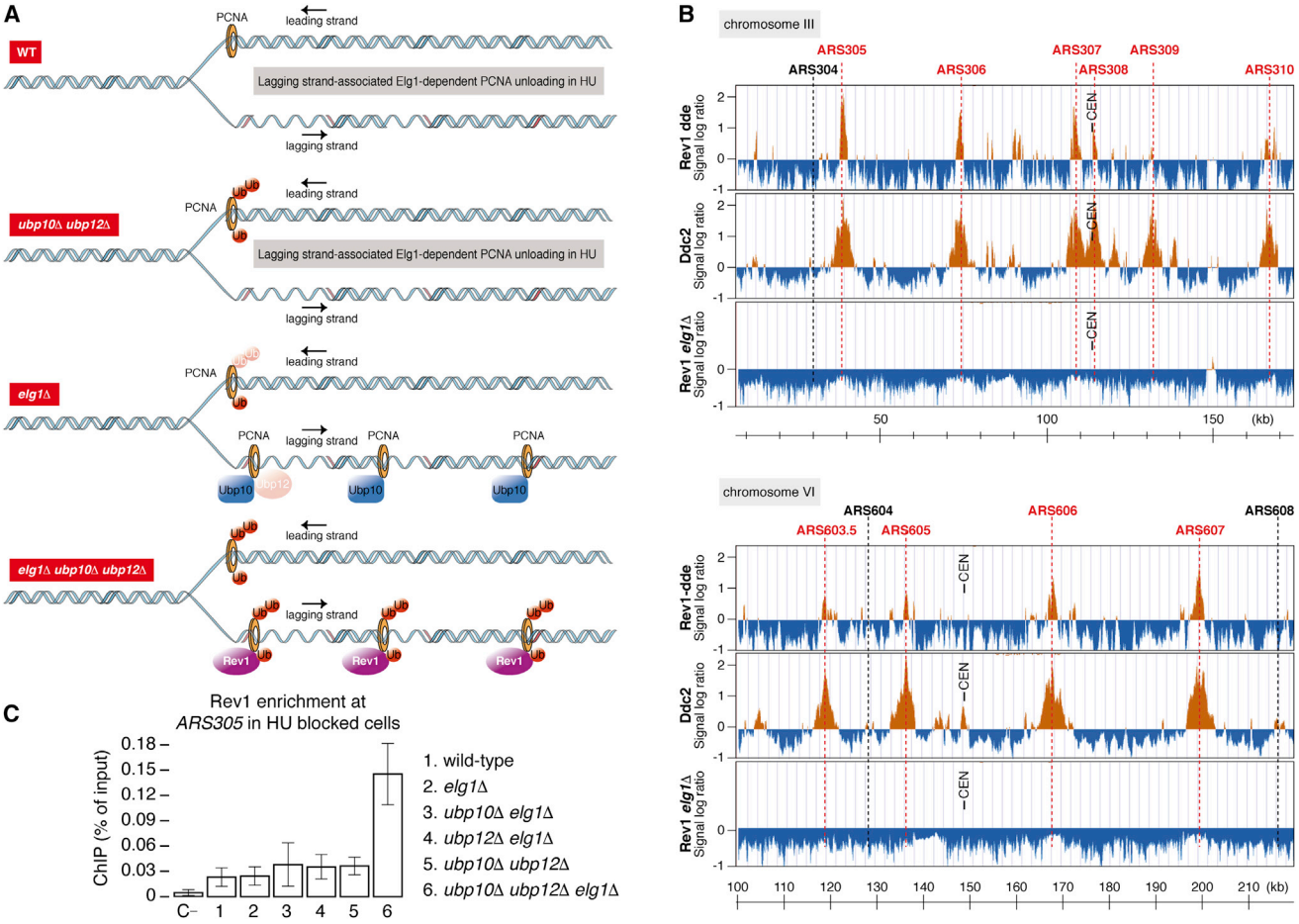

Figure 5. TLS Polymerase ζ-Associated Rev1 Protein Binding to Replication Forks Is Counteracted by PCNA-DUBs and Lagging-Strand PCNA Unloading

(A) Analysis of TLS polymerase ζ-associated Rev1 localization to sites of active DNA replication by ChIP-on-chip and ChIP-qPCR.

(B) ChIP-on-chip analysis of *REV1-myc ubp10Δ ubp12Δ elg1Δ* (Rev1 dde), *DDC2-myc* (Ddc2), and *REV1-myc elg1Δ* (Rev1 *elg1Δ*) cells pre-synchronized with α-factor and released for 1 h in the presence of 0.2 M HU. Orange histogram bars on the y axis show the average signal ratio of loci significantly enriched in each immunoprecipitated fraction in $\log_2$ scale. The x axis shows chromosomal coordinated in kilobases along regions in chromosomes III and VI. Early-firing (in red) and late/dormant (in black) replication origins are shown. Positions of early-firing origins are indicated by dotted red lines. Centromere (CEN) positions are shown.

(C) ChIP-qPCR analysis of Rev1 enrichment at *ARS305* in the indicated cells upon release from G1 into 0.2 M HU.

Means and SDs of three independent experiments are shown.

in conjunction with Ubp10 to deubiquitylate PCNA in the S phase. We report that Ubp10 and Ubp12 associate with replication forks and that in their absence, TS and TLS events are exacerbated at sites of DNA synthesis, suggesting that PCNA deubiquitylation at replication forks serves DDT regulation, as opposed to simply mediating PCNA recycling.

In eukaryotes, cells mutated in $PCNA^{K164}$ or lacking the Rad18 ubiquitin ligase are hypersensitive to alkylating damage induced by MMS, reflecting the pivotal role played by ubiquitylation of this residue in activating pathways that bypass DNA lesions to promote cell viability (Hoege et al., 2002; Stelter and Ulrich, 2003). We show here that the ablation of Ubp10 or Ubp12 results in an accumulation of ubiquitylated PCNA, and, conversely, overexpression of either DUB determines a reduction in PCNA ubiquitylation in response to genotoxic agents. Hence, the sensitivity to MMS conferred by DUB overexpression is likely due to a failure in achieving PCNA ubiquitylation levels necessary to trigger lesion bypass mechanisms. We note that Ubp10-overexpressing cells are more sensitive to MMS than those overproducing Ubp12, suggesting that Ubp10 may act as the main PCNA deubiquitylase in budding yeast. Nonetheless, ablation of Ubp10 results in an accumulation of ubiquitylated PCNA forms following exposure to DNA damage or replication blocks (Gallego-Sánchez et al., 2012), while elimination of Ubp12 only enhances the accumulation of Ub- and Ub_2-$PCNA^{K164}$ in Ubp10-defective cells, suggesting that DUBs functionally overlap and that Ubp12 can take over some of Ubp10 roles in its absence (e.g., suppressing Rev1 binding to forks in *ubp10Δ* cells). Strikingly, ubiquitylated PCNA is robustly detected in *ubp10 ubp12* double mutants during unperturbed replication.

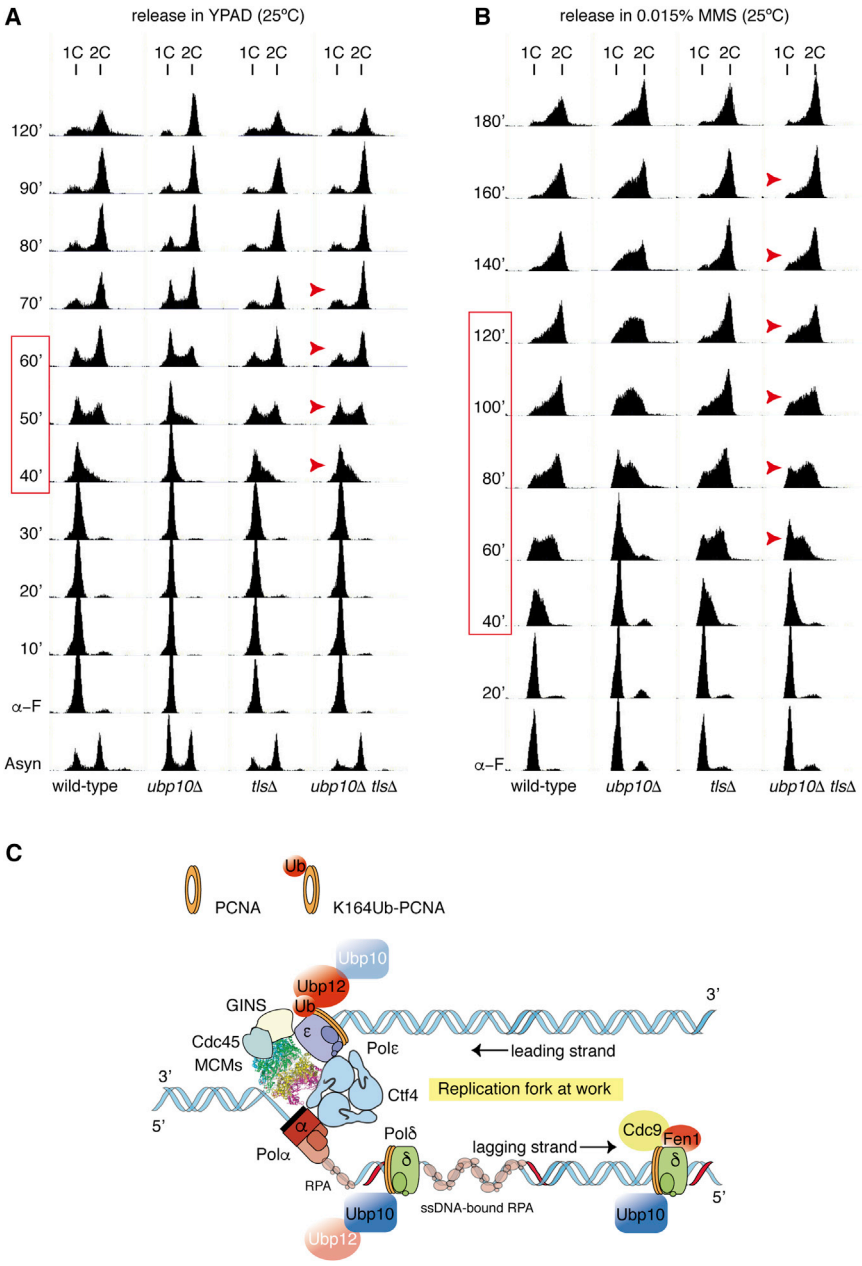

Figure 6. TLS DNA-Polymerases Determine Replication Progression Defects in *ubp10Δ* Cells

(A and B) DNA content analysis of wild-type, *ubp10Δ*, *rev1Δ rev3Δ rad30Δ* (*tlsΔ*), and *ubp10Δ rev1Δ rev3Δ rad30Δ* (*ubp10Δ tlsΔ*) strains. Cells were synchronized with α-factor and released in fresh yeast complex media (YPAD; unperturbed conditions) (A) or in 0.015% MMS YPAD (damage conditions) (B). The progression of the bulk genome replication was monitored at the indicated time points by FACS. Red boxes indicate approximate S-phase duration in wild-type cells. Red arrows indicate time points in which *tlsΔ* suppresses the replication defect of *ubp10Δ* cells.

(C) Hypothetical model for DDT suppression at replication forks through Ubp10- and Ubp12-mediated PCNA deubiquitylation (see text for details).

We contend that spontaneous DNA lesions, likely due to endogenous damage, or futile Rad6/Rad18 activation may account for such PCNA ubiquitylation in the absence of genotoxic stimuli; these are therefore likely to underlie chromosome replication defects owing to DDT enhancement in PCNA-DUB *ubp10* mutants. However, Ubp10 and Ubp12 exhibit diverse preferences for ubiquitin-chain removal, a remarkable characteristic of the *in vivo* enzymatic activity of PCNA^{K164}-ubiquitin proteases. Indeed, Ubp10 and Ubp12 preferences for completely deubiquitylating PCNA or removing polyubiquitin chains, respectively, suggest that these enzymes are likely not just to primarily back up each other, but also to play dedicated roles in damage bypass control.

It will be interesting to investigate if additional PCNA-DUBs operate in yeast cells, which could add further layers of complexity to DDT regulation at replication forks, and if an equivalent enzymatic diversity and cooperation between editors of PCNA ubiquitin chains also occurs in human cells.

We show here that the enzymes driving PCNA^{K164} deubiquitylation downregulate DDT events at replication forks. First, Rad52-dependent replication intermediate transitions, consistent with the engagement of nascent strands in TS events, accumulate in PCNA-DUB-deficient cells when forks negotiate damaged templates or dNTPs shortage. X-shaped TS intermediates accumulate during the replication of alkylated DNA, owing to nascent strand exchange events mediated by Rad52, which lead to joint molecules primarily dissolved by the Sgs1 RecQ family helicase (Giannattasio et al., 2014; González-Prieto et al., 2013; Liberi et al., 2005; Lopes et al., 2003; Mankouri and Hickson, 2006). Accumulation of these molecules in PCNA-DUB mutants is likely the consequence of a lack of leverage on the activity of PCNA^{K164} ubiquitin ligases, resulting in an overall increase of PCNA poly-ubiquitylation, presumably close to polymerase-blocking lesions. Of particular interest is the accumulation of non-canonical molecules in HU-treated PCNA-DUB mutants. These intermediates are Rad52 dependent and are observed upon DUBs ablation only, suggesting that they represent transitions engaging nascent strands that are normally suppressed by PCNA deubiquitylation. The migration properties of these intermediates on 2D gels are indicative of a Y-shaped structure and a mass lower than fully replicated molecules, the

latter suggesting an incomplete synthesis of the nascent strands. This fact, together with the observation that these molecules accumulate at the expense of canonical large Y-shaped intermediates, suggests that they might arise from TS attempts by nascent strands close to sites of replicative polymerase stalling. Further work will be required to analyze the precise molecular nature and functional meaning of these intermediates.

In addition, binding of the TLS polymerase ζ-associated Rev1 protein to stalled replication forks is also increased upon the ablation of Ubp10 and Ubp12 DUBs, along with the RFC PCNA unloader Elg1 subunit. Rev1 plays a role in Rev3–Rev7 (TLS Polymerase ζ) complex formation (Haracska et al., 2001; Nelson et al., 1996). Hence, PCNA-DUBs counteract the fork recruitment, and presumably the function, of the Polymerase ζ TLS polymerase, most likely resulting in a downregulation of error-prone lesion bypass. As mentioned, $PCNA^{K164}$ ubiquitylation occurs in S phase in yeast and other model systems (Álvarez et al., 2016; Daigaku et al., 2010, 2017; Davies et al., 2008; Hoege et al., 2002; Huang et al., 2006; Stelter and Ulrich, 2003), and Rad18 $PCNA^{K164}$-E3-ubiquitin ligase binding to forks is promoted by the presence of RPA-coated ssDNA (Davies et al., 2008). PCNA ubiquitylation can be genetically forced to occur after genome replication without impairing genome integrity or cell viability (Daigaku et al., 2010; Karras and Jentsch, 2010), which raised the notion that lesion bypass may work primarily as a repair mechanism acting on ssDNA gaps, persisting after the completion of bulk damaged chromosome replication (Karras and Jentsch, 2010). Our findings suggest that the reversion of PCNA ubiquitylation by Upb10 and Ubp12 DUBs represents a key regulatory layer to limit fork engagement in DDT mechanisms. This raises the possibility that in certain circumstances, cells might resort to "on the fly" lesion bypass in the context of replication forks, though such a co-replicative mechanism would be constitutively downregulated by DUB-mediated PCNA deubiquitylation.

The PCNA-ubiquitin ligase Rad18, the FANCD2/PCNA-DUB USP1, and TLS DNA polymerase η associate with sites of DNA synthesis, along with replisome factors in mammalian cells (Despras et al., 2016; Dungrawala et al., 2015; Kile et al., 2015). In line with these observations, we report that yeast Ubp10 and Ubp12 PCNA-DUBs associate with replication forks in unperturbed conditions. However, upon fork stalling Upb10, but not Ubp12, binding to forks is counteracted by Elg1, a factor that unloads PCNA from lagging strands (Kubota et al., 2013, 2015; Yu et al., 2014). It has been estimated that two PCNA molecules are present at lagging strands per each complex present at leading strands (Yu et al., 2014), and, owing to defective unloading from lagging strands, PCNA detection at stalled forks increases in Elg1-ablated cells (Kubota et al., 2013, 2015; Yu et al., 2014). Nonetheless, PCNA is detectable at stalled forks in wild-type cells, as a fraction of clamp loader molecules remains associated with leading strands (Yu et al., 2014). In contrast to PCNA, we failed to observe the Ubp10 association with stalled forks in *ELG1* wild-type cells, arguing that Ubp10 is likely absent from leading strands. In agreement with the inferred preferential lagging-strand association of Ubp10, coIP analysis evidenced that Ubp10, but not Ubp12, interacts with the Okazaki-fragment processing factor Fen1/Rad27, acting exclusively during the last steps of lagging-strand synthesis (Figure S6E). In contrast, Ubp12 association with replication forks in HU-treated cells is not influenced by the presence of a functional Elg1, suggesting that it might primarily associate with leading-strand PCNA.

We envision, based on these observations, that PCNA-DUBs might asymmetrically associate with nascent DNA strands (Figure 6C). This, taken together with the distinct preference of the two DUBs for PCNA deubiquitylation, might establish a framework for differential PCNA deubiquitylation and handling of lesion bypass at leading- or lagging-strand templates. Though further work will be required to firmly establish this notion, it is tantalizing to speculate that the substrate preference of Ubp10 may favor full PCNA deubiquitylation at lagging strands and that, conversely, Ubp12 may preferentially deconjugate K63-linked ubiquitin moieties, permitting the residence of mono-ubiquitylated PCNA at leading strands. In this scenario, leading strands may be relatively permissive for engagement in TLS events owing to the presence of mono-ubiquitylated PCNA. Instead, both DDT pathways might be counteracted at lagging strands, as a consequence of full PCNA deubiquitylation and, in the case of HU-induced fork stalling, PCNA unloading.

The evidence presented here argues that PCNA-DUBs revert PCNA ubiquitylation to limit lesion bypass events in the environment of replication forks, raising the key question of what the biological meaning of DDT suppression is during replication. An obvious option is that the extension of DDT events requires limitation in order to avoid increased mutagenesis or excessive sister chromatid junctions owing to TLS and TS events, respectively. In addition, the presence of PCNA-ubiquitin ligases at replication forks might lead to unscheduled ubiquitylation of the replicative clamp, which may in turn trigger futile bypass events encumbering the progression of replication machineries. In this respect, we found that the ablation of TLS polymerases alleviates the replication defects of *ubp10* mutants, suggesting that an exacerbation of TLS polymerase recruitment might basally hamper a processive function of replicative polymerases.

In light of our findings, we propose that fork-associated Ubp10 and Ubp12 revert $PCNA^{K164}$ ubiquitylation to restrain DDT at nascent DNA, likely to limit the extension and deleterious impact of lesion bypass events, and, in doing so, facilitate a processive replication of chromosomal DNA.

STAR★METHODS

Detailed methods are provided in the online version of this paper and include the following:

- KEY RESOURCES TABLE
- LEAD CONTACT AND MATERIALS AVAILABILITY
- EXPERIMENTAL MODEL AND SUBJECT DETAILS
  - Yeast Strains
- METHOD DETAILS
  - General Experimental Procedures and Flow Cytometry
  - MMS and HU Sensitivity Assays
  - Tagging Yeast Proteins and Gene Deletion

SUPPLEMENTAL INFORMATION

Supplemental Information can be found online at https://doi.org/10.1016/j.celrep.2019.09.054.

ACKNOWLEDGMENTS

We are grateful to the B08 group at the IBMCC for helpful discussions. This work was supported by the Spanish Ministry of Science (grants BFU2017-87013-R to R.B. and BFU2015-69709-P to A.B. and M.P.S.) and Junta de Castilla y León (grant SA042P17 to A.B.). A.B.'s institution is supported by the "Programa de Apoyo a Planes Estratégicos de Investigación de Excelencia" cofunded by the Junta de Castilla y León and the European Regional Development Fund (CLC-2017-01).

AUTHOR CONTRIBUTIONS

Conceptualization, A.B., with substantial inputs from R.B. and M.P.S.; Methodology, A.B. and R.B.; Validation, A.B., V.Á., M.P.S., and R.B.; Formal Analysis, A.B., V.Á., M.P.S., and R.B.; Investigation, V.Á., C.F., M.P.S., A.G.-S., R.B., and A.B.; Resources, V.Á., A.G.-S., R.B., and A.B.; Writing – Original Draft, A.B.; Writing – Review & Editing, A.B., M.P.S., and R.B.; Visualization, A.B.; Supervision, A.B., M.P.S., and R.B.; Funding Acquisition, A.B., M.P.S., and R.B.

DECLARATION OF INTERESTS

The authors declare no competing interests.

Received: March 25, 2019
Revised: August 1, 2019
Accepted: September 17, 2019
Published: October 29, 2019

REFERENCES

Alabert, C., Bukowski-Wills, J.-C., Lee, S.-B., Kustatscher, G., Nakamura, K., de Lima Alves, F., Menard, P., Mejlvang, J., Rappsilber, J., and Groth, A. (2014). Nascent chromatin capture proteomics determines chromatin dynamics during DNA replication and identifies unknown fork components. Nat. Cell Biol. *16*, 281–293.

Álvarez, V., Viñas, L., Gallego-Sánchez, A., Andrés, S., Sacristán, M.P., and Bueno, A. (2016). Orderly progression through S-phase requires dynamic ubiquitylation and deubiquitylation of PCNA. Sci. Rep. *6*, 25513.

Ang, J.S., Duffy, S., Segovia, R., Stirling, P.C., and Hieter, P. (2016). Dosage Mutator Genes in Saccharomyces cerevisiae: A Novel Mutator Mode-of-Action of the Mph1 DNA Helicase. Genetics *204*, 975–986.

Arakawa, H., Moldovan, G.L., Saribasak, H., Saribasak, N.N., Jentsch, S., and Buerstedde, J.M. (2006). A role for PCNA ubiquitination in immunoglobulin hypermutation. PLoS Biol. *4*, e366.

Ben-Aroya, S., Koren, A., Liefshitz, B., Steinlauf, R., and Kupiec, M. (2003). ELG1, a yeast gene required for genome stability, forms a complex related to replication factor C. Proc. Natl. Acad. Sci. USA *100*, 9906–9911.

Bergink, S., and Jentsch, S. (2009). Principles of ubiquitin and SUMO modifications in DNA repair. Nature *458*, 461–467.

Bermejo, R., Doksani, Y., Capra, T., Katou, Y.-M., Tanaka, H., Shirahige, K., and Foiani, M. (2007). Top1- and Top2-mediated topological transitions at replication forks ensure fork progression and stability and prevent DNA damage checkpoint activation. Genes Dev. *21*, 1921–1936.

Bermejo, R., Capra, T., Gonzalez-Huici, V., Fachinetti, D., Cocito, A., Natoli, G., Katou, Y., Mori, H., Kurokawa, K., Shirahige, K., and Foiani, M. (2009a). Genome-organizing factors Top2 and Hmo1 prevent chromosome fragility at sites of S phase transcription. Cell *138*, 870–884.

Bermejo, R., Katou, Y.-M., Shirahige, K., and Foiani, M. (2009b). ChIP-on-chip analysis of DNA topoisomerases. Methods Mol. Biol. *582*, 103–118.

Bernstein, K.A., Shor, E., Sunjevaric, I., Fumasoni, M., Burgess, R.C., Foiani, M., Branzei, D., and Rothstein, R. (2009). Sgs1 function in the repair of DNA replication intermediates is separable from its role in homologous recombinational repair. EMBO J. *28*, 915–925.

Borodovsky, A., Kessler, B.M., Casagrande, R., Overkleeft, H.S., Wilkinson, K.D., and Ploegh, H.L. (2001). A novel active site-directed probe specific for deubiquitylating enzymes reveals proteasome association of USP14. EMBO J. *20*, 5187–5196.

Branzei, D. (2011). Ubiquitin family modifications and template switching. FEBS Lett. *585*, 2810–2817.

Branzei, D., and Foiani, M. (2010). Maintaining genome stability at the replication fork. Nat. Rev. Mol. Cell Biol. *11*, 208–219.

Calzada, A., Sánchez, M., Sánchez, E., and Bueno, A. (2000). The stability of the Cdc6 protein is regulated by cyclin-dependent kinase/cyclin B complexes in Saccharomyces cerevisiae. J. Biol. Chem. *275*, 9734–9741.

Calzada, A., Sacristán, M., Sánchez, E., and Bueno, A. (2001). Cdc6 cooperates with Sic1 and Hct1 to inactivate mitotic cyclin-dependent kinases. Nature *412*, 355–358.

Calzada, A., Hodgson, B., Kanemaki, M., Bueno, A., and Labib, K. (2005). Molecular anatomy and regulation of a stable replisome at a paused eukaryotic DNA replication fork. Genes Dev. *19*, 1905–1919.

Chang, D.J., and Cimprich, K.A. (2009). DNA damage tolerance: when it's OK to make mistakes. Nat. Chem. Biol. *5*, 82–90.

Chang, D.J., Lupardus, P.J., and Cimprich, K.A. (2006). Monoubiquitination of proliferating cell nuclear antigen induced by stalled replication requires uncoupling of DNA polymerase and mini-chromosome maintenance helicase activities. J. Biol. Chem. *281*, 32081–32088.

Cordón-Preciado, V., Ufano, S., and Bueno, A. (2006). Limiting amounts of budding yeast Rad53 S-phase checkpoint activity results in increased resistance to DNA alkylation damage. Nucleic Acids Res. *34*, 5852–5862.

Daigaku, Y., Davies, A.A., and Ulrich, H.D. (2010). Ubiquitin-dependent DNA damage bypass is separable from genome replication. Nature *465*, 951–955.

Daigaku, Y., Etheridge, T.J., Nakazawa, Y., Nakayama, M., Watson, A.T., Miyabe, I., Ogi, T., Osborne, M.A., and Carr, A.M. (2017). PCNA ubiquitylation ensures timely completion of unperturbed DNA replication in fission yeast. PLoS Genet. *13*, e1006789.

Davies, A.A., Huttner, D., Daigaku, Y., Chen, S., and Ulrich, H.D. (2008). Activation of ubiquitin-dependent DNA damage bypass is mediated by replication protein a. Mol. Cell *29*, 625–636.

Despras, E., Sittewelle, M., Pouvelle, C., Delrieu, N., Cordonnier, A.M., and Kannouche, P.L. (2016). Rad18-dependent SUMOylation of human specialized DNA polymerase eta is required to prevent under-replicated DNA. Nat. Commun. *7*, 13326.

Dungrawala, H., Rose, K.L., Bhat, K.P., Mohni, K.N., Glick, G.G., Couch, F.B., and Cortez, D. (2015). The Replication Checkpoint Prevents Two Types of Fork Collapse without Regulating Replisome Stability. Mol. Cell *59*, 998–1010.

Emre, N.C.T., Ingvarsdottir, K., Wyce, A., Wood, A., Krogan, N.J., Henry, K.W., Li, K., Marmorstein, R., Greenblatt, J.F., Shilatifard, A., and Berger, S.L. (2005). Maintenance of low histone ubiquitylation by Ubp10 correlates with telomere-proximal Sir2 association and gene silencing. Mol. Cell *17*, 585–594.

Frampton, J., Irmisch, A., Green, C.M., Neiss, A., Trickey, M., Ulrich, H.D., Furuya, K., Watts, F.Z., Carr, A.M., and Lehmann, A.R. (2006). Postreplication repair and PCNA modification in Schizosaccharomyces pombe. Mol. Biol. Cell *17*, 2976–2985.

Frattini, C., Villa-Hernández, S., Pellicanò, G., Jossen, R., Katou, Y., Shirahige, K., and Bermejo, R. (2017). Cohesin Ubiquitylation and Mobilization Facilitate Stalled Replication Fork Dynamics. Mol. Cell *68*, 758–772.e4.

Friedberg, E.C. (2005). Suffering in silence: the tolerance of DNA damage. Nat. Rev. Mol. Cell Biol. *6*, 943–953.

Friedberg, E.C., and Gerlach, V.L. (1999). Novel DNA polymerases offer clues to the molecular basis of mutagenesis. Cell *98*, 413–416.

Gallego-Sánchez, A., Andrés, S., Conde, F., San-Segundo, P.A., and Bueno, A. (2012). Reversal of PCNA ubiquitylation by Ubp10 in Saccharomyces cerevisiae. PLoS Genet. *8*, e1002826.

Gallo, D., Kim, T., Szakal, B., Saayman, X., Narula, A., Park, Y., Branzei, D., Zhang, Z., and Brown, G.W. (2019). Rad5 recruits error-prone DNA polymerases for mutagenic repair of ssDNA gaps on undamaged templates. Mol. Cell *73*, 900–914.e9.

Gardner, R.G., Nelson, Z.W., and Gottschling, D.E. (2005). Ubp10/Dot4p regulates the persistence of ubiquitinated histone H2B: distinct roles in telomeric silencing and general chromatin. Mol. Cell. Biol. *25*, 6123–6139.

Garg, P., and Burgers, P.M. (2005). Ubiquitinated proliferating cell nuclear antigen activates translesion DNA polymerases eta and REV1. Proc. Natl. Acad. Sci. USA *102*, 18361–18366.

Ghosal, G., and Chen, J. (2013). DNA damage tolerance: a double-edged sword guarding the genome. Transl. Cancer Res. *2*, 107–129.

Giannattasio, M., Zwicky, K., Follonier, C., Foiani, M., Lopes, M., and Branzei, D. (2014). Visualization of recombination-mediated damage bypass by template switching. Nat. Struct. Mol. Biol. *21*, 884–892.

González-Prieto, R., Muñoz-Cabello, A.M., Cabello-Lobato, M.J., and Prado, F. (2013). Rad51 replication fork recruitment is required for DNA damage tolerance. EMBO J. *32*, 1307–1321.

Haase, S.B. (2004). Cell cycle analysis of budding yeast using SYTOX Green. Curr. Protoc. Cytom. *26*, 7.23.1–7.23.4.

Haase, S.B., and Reed, S.I. (2002). Improved flow cytometric analysis of the budding yeast cell cycle. Cell Cycle *1*, 132–136.

Haracska, L., Unk, I., Johnson, R.E., Johansson, E., Burgers, P.M., Prakash, S., and Prakash, L. (2001). Roles of yeast DNA polymerases delta and zeta and of Rev1 in the bypass of abasic sites. Genes Dev. *15*, 945–954.

Haracska, L., Unk, I., Prakash, L., and Prakash, S. (2006). Ubiquitylation of yeast proliferating cell nuclear antigen and its implications for translesion DNA synthesis. Proc. Natl. Acad. Sci. USA *103*, 6477–6482.

Hedglin, M., and Benkovic, S.J. (2015). Regulation of Rad6/Rad18 Activity During DNA Damage Tolerance. Annu. Rev. Biophys. *44*, 207–228.

Hoege, C., Pfander, B., Moldovan, G.L., Pyrowolakis, G., and Jentsch, S. (2002). RAD6-dependent DNA repair is linked to modification of PCNA by ubiquitin and SUMO. Nature *419*, 135–141.

Huang, T.T., Nijman, S.M.B., Mirchandani, K.D., Galardy, P.J., Cohn, M.A., Haas, W., Gygi, S.P., Ploegh, H.L., Bernards, R., and D'Andrea, A.D. (2006). Regulation of monoubiquitinated PCNA by DUB autocleavage. Nat. Cell Biol. *8*, 339–347.

Hutter, K.J., and Eipel, H.E. (1979). Microbial determinations by flow cytometry. J. Gen. Microbiol. *113*, 369–375.

Jossen, R., and Bermejo, R. (2013). The DNA damage checkpoint response to replication stress: A Game of Forks. Front. Genet. *4*, 26.

Kannouche, P.L., Wing, J., and Lehmann, A.R. (2004). Interaction of human DNA polymerase eta with monoubiquitinated PCNA: a possible mechanism for the polymerase switch in response to DNA damage. Mol. Cell *14*, 491–500.

Karras, G.I., and Jentsch, S. (2010). The RAD6 DNA damage tolerance pathway operates uncoupled from the replication fork and is functional beyond S phase. Cell *141*, 255–267.

Katou, Y., Kanoh, Y., Bando, M., Noguchi, H., Tanaka, H., Ashikari, T., Sugimoto, K., and Shirahige, K. (2003). S-phase checkpoint proteins Tof1 and Mrc1 form a stable replication-pausing complex. Nature *424*, 1078–1083.

Kile, A.C., Chavez, D.A., Bacal, J., Eldirany, S., Korzhnev, D.M., Bezsonova, I., Eichman, B.F., and Cimprich, K.A. (2015). HLTF's Ancient HIRAN Domain Binds 3′ DNA Ends to Drive Replication Fork Reversal. Mol. Cell *58*, 1090–1100.

Kubota, T., Nishimura, K., Kanemaki, M.T., and Donaldson, A.D. (2013). The Elg1 replication factor C-like complex functions in PCNA unloading during DNA replication. Mol. Cell *50*, 273–280.

Kubota, T., Katou, Y., Nakato, R., Shirahige, K., and Donaldson, A.D. (2015). Replication-Coupled PCNA Unloading by the Elg1 Complex Occurs Genome-wide and Requires Okazaki Fragment Ligation. Cell Rep. *12*, 774–787.

Lawrence, C. (1994). The RAD6 DNA repair pathway in Saccharomyces cerevisiae: what does it do, and how does it do it? BioEssays *16*, 253–258.

Leach, C.A., and Michael, W.M. (2005). Ubiquitin/SUMO modification of PCNA promotes replication fork progression in Xenopus laevis egg extracts. J. Cell Biol. *171*, 947–954.

Liberi, G., Maffioletti, G., Lucca, C., Chiolo, I., Baryshnikova, A., Cotta-Ramusino, C., Lopes, M., Pellicioli, A., Haber, J.E., and Foiani, M. (2005). Rad51-dependent DNA structures accumulate at damaged replication forks in sgs1 mutants defective in the yeast ortholog of BLM RecQ helicase. Genes Dev. *19*, 339–350.

Longhese, M.P., Paciotti, V., Fraschini, R., Zaccarini, R., Plevani, P., and Lucchini, G. (1997). The novel DNA damage checkpoint protein ddc1p is phosphorylated periodically during the cell cycle and in response to DNA damage in budding yeast. EMBO J. *16*, 5216–5226.

Longtine, M.S., McKenzie, A., 3rd, Demarini, D.J., Shah, N.G., Wach, A., Brachat, A., Philippsen, P., and Pringle, J.R. (1998). Additional modules for versatile and economical PCR-based gene deletion and modification in Saccharomyces cerevisiae. Yeast *14*, 953–961.

Lopes, M., Cotta-Ramusino, C., Pellicioli, A., Liberi, G., Plevani, P., Muzi-Falconi, M., Newlon, C.S., and Foiani, M. (2001). The DNA replication checkpoint response stabilizes stalled replication forks. Nature *412*, 557–561.

Lopes, M., Cotta-Ramusino, C., Liberi, G., and Foiani, M. (2003). Branch migrating sister chromatid junctions form at replication origins through Rad51/Rad52-independent mechanisms. Mol. Cell *12*, 1499–1510.

Lucca, C., Vanoli, F., Cotta-Ramusino, C., Pellicioli, A., Liberi, G., Haber, J., and Foiani, M. (2004). Checkpoint-mediated control of replisome-fork association and signalling in response to replication pausing. Oncogene *23*, 1206–1213.

Mailand, N., Gibbs-Seymour, I., and Bekker-Jensen, S. (2013). Regulation of PCNA-protein interactions for genome stability. Nat. Rev. Mol. Cell Biol. *14*, 269–282.

Mankouri, H.W., and Hickson, I.D. (2006). Top3 processes recombination intermediates and modulates checkpoint activity after DNA damage. Mol. Biol. Cell *17*, 4473–4483.

Nelson, J.R., Lawrence, C.W., and Hinkle, D.C. (1996). Deoxycytidyl transferase activity of yeast REV1 protein. Nature *382*, 729–731.

Niimi, A., Brown, S., Sabbioneda, S., Kannouche, P.L., Scott, A., Yasui, A., Green, C.M., and Lehmann, A.R. (2008). Regulation of proliferating cell nuclear antigen ubiquitination in mammalian cells. Proc. Natl. Acad. Sci. USA *105*, 16125–16130.

Park, J.M., Yang, S.W., Yu, K.R., Ka, S.H., Lee, S.W., Seol, J.H., Jeon, Y.J., and Chung, C.H. (2014). Modification of PCNA by ISG15 plays a crucial role in termination of error-prone translesion DNA synthesis. Mol. Cell *54*, 626–638.

Raghuraman, M.K., Winzeler, E.A., Collingwood, D., Hunt, S., Wodicka, L., Conway, A., Lockhart, D.J., Davis, R.W., Brewer, B.J., and Fangman, W.L. (2001). Replication dynamics of the yeast genome. Science *294*, 115–121.

Sánchez, M., Calzada, A., and Bueno, A. (1999). The Cdc6 protein is ubiquitinated in vivo for proteolysis in Saccharomyces cerevisiae. J. Biol. Chem. *274*, 9092–9097.

Santocanale, C., and Diffley, J.F. (1998). A Mec1- and Rad53-dependent checkpoint controls late-firing origins of DNA replication. Nature *395*, 615–618.

Schulze, J.M., Hentrich, T., Nakanishi, S., Gupta, A., Emberly, E., Shilatifard, A., and Kobor, M.S. (2011). Splitting the task: Ubp8 and Ubp10 deubiquitinate different cellular pools of H2BK123. Genes Dev. *25*, 2242–2247.

Shirahige, K., Hori, Y., Shiraishi, K., Yamashita, M., Takahashi, K., Obuse, C., Tsurimoto, T., and Yoshikawa, H. (1998). Regulation of DNA-replication origins during cell-cycle progression. Nature *395*, 618–621.

Sollier, J., Driscoll, R., Castellucci, F., Foiani, M., Jackson, S.P., and Branzei, D. (2009). The Saccharomyces cerevisiae Esc2 and Smc5-6 proteins promote sister chromatid junction-mediated intra-S repair. Mol. Biol. Cell *20*, 1671–1682.

Stelter, P., and Ulrich, H.D. (2003). Control of spontaneous and damage-induced mutagenesis by SUMO and ubiquitin conjugation. Nature *425*, 188–191.

Tercero, J.A., and Diffley, J.F. (2001). Regulation of DNA replication fork progression through damaged DNA by the Mec1/Rad53 checkpoint. Nature *412*, 553–557.

Ulrich, H.D. (2006). Deubiquitinating PCNA: a downside to DNA damage tolerance. Nat. Cell Biol. *8*, 303–305.

Ulrich, H.D. (2009). Regulating post-translational modifications of the eukaryotic replication clamp PCNA. DNA Repair (Amst.) *8*, 461–469.

Ulrich, H.D. (2011). Timing and spacing of ubiquitin-dependent DNA damage bypass. FEBS Lett. *585*, 2861–2867.

Vanoli, F., Fumasoni, M., Szakal, B., Maloisel, L., and Branzei, D. (2010). Replication and recombination factors contributing to recombination-dependent bypass of DNA lesions by template switch. PLoS Genet. *6*, e1001205.

Watanabe, K., Tateishi, S., Kawasuji, M., Tsurimoto, T., Inoue, H., and Yamaizumi, M. (2004). Rad18 guides poleta to replication stalling sites through physical interaction and PCNA monoubiquitination. EMBO J. *23*, 3886–3896.

Wyrick, J.J., Aparicio, J.G., Chen, T., Barnett, J.D., Jennings, E.G., Young, R.A., Bell, S.P., and Aparicio, O.M. (2001). Genome-wide distribution of ORC and MCM proteins in S. cerevisiae: high-resolution mapping of replication origins. Science *294*, 2357–2360.

Yu, C., Gan, H., Han, J., Zhou, Z.-X., Jia, S., Chabes, A., Farrugia, G., Ordog, T., and Zhang, Z. (2014). Strand-specific analysis shows protein binding at replication forks and PCNA unloading from lagging strands when forks stall. Mol. Cell *56*, 551–563.

Zhang, H., and Lawrence, C.W. (2005). The error-free component of the RAD6/RAD18 DNA damage tolerance pathway of budding yeast employs sister-strand recombination. Proc. Natl. Acad. Sci. USA *102*, 15954–15959.

Zou, L., and Elledge, S.J. (2003). Sensing DNA damage through ATRIP recognition of RPA-ssDNA complexes. Science *300*, 1542–1548.

STAR★METHODS

KEY RESOURCES TABLE

REAGENT or RESOURCE	SOURCE	IDENTIFIER
Antibodies		
Mouse anti-Flag (M2)	Sigma-Aldrich	Cat#F1804; RRID:AB_259529
Anti-HA (12CA5)	Roche	Cat#11666606001; RRID:AB_514506
Anti-Myc Tag (9E10)	Sigma-Aldrich	Cat#M5546: RRID:AB_439695
Anti PK Anti-V5 Tag (E10/V4RR)	Thermo Fisher	Cat#MA5-15253; RRID:AB_2537639
Anti-Myc-HRP	Miltenyi Biotech	Cat#120-002-532; RRID:AB_871937
Anti-PCNA rabbit polyclonal	Dr. Kaufmann's Lab	N/A
Anti-Clb2	Santa Cruz Biotech	Cat#SC-9071; RRID:AB_667962
Anti-Clb5	Santa Cruz Biotech	Cat#SC-20170; RRID:AB_671845
Anti-Sic1	Santa Cruz Biotech	Cat#SC-50441; RRID:AB_785671
Anti-PGK	Molecular Probes	Cat#A-6457;RRID:AB_221541
Anti-Mouse-HRP	GE Healthcare	Cat#NXA931V; RRID:AB_2721110
Anti-Rabbit-HRP	GE Healthcare	Cat#NA934V; RRID:AB_772191
Chemicals, Peptides, and Recombinant Proteins		
Raffinose	Sigma-Aldrich	Cat#R0250
Galactose	Sigma-Aldrich	Cat#G0750
RNase A	Sigma-Aldrich	Cat#R5503
Proteinase K	Roche	Cat#03115852001
Hydroxyurea	Ibian Tecnologies	Cat#HDU0250
Complete Protease Inhibitor-EDTA free	Roche	Cat#11873580001
Dynabeads Protein-G	Life Tecnologies	Cat#10765583
Methyl Methanesulfonate	Sigma-Aldrich	Cat#129925
Canavanine	Sigma-Aldrich	Cat#C9758
SYTOX Green	Invitrogen	Cat#S7020
Alpha-factor Mating Pheromone	GenSCRIPT	Cat#RP01002
Ubiquitin Vinyl Sulfone (UbVS)	Enzo Life Sciences	Cat#BML-UW155-0025
Spermine	Sigma-Aldrich	Cat#S1141
Spermidine	Sigma-Aldrich	Cat#S2501
Phenol/Chlorophorm/Isoamylalcohol pH 8.0	Sigma-Aldrich	Cat#P4803
Formaldehyde	Sigma-Aldrich	Cat#F8775
Amersham Hybond-XL	GE Healthcare	Cat#RPN203S
QIAGEN Genomic-Tips 100/G	QIAGEN	Cat#50910243
Illustra Microspin G-50 columns	GE Healthcare	Cat#11753309
Critical Commercial Assays		
QIAquick PCR purification kit	QIAGEN	Cat#28106
iQ-SYBRE Green supermix	Bio-Rad	Cat#1708882
Prime-a-Gene® Labeling System	Promega	Cat#U1100
Deposited Data		
Microarray data	This paper	GSE90157
Experimental Models: Organisms/Strains		
Saccharomyces cerevisiae W303 *Mat**a** ade2-1 can1-100 his3-11,15 leu2-3,112 trp1-1 ura3-1 RAD5 bar1Δ::LEU2*	Lab stock	55.34
55.34 with ubp10::hphMX4	Lab stock	61.33
55.34 with ubp12::kanMX	Lab stock	69.03

(*Continued on next page*)

Continued

REAGENT or RESOURCE	SOURCE	IDENTIFIER
55.34 with ubp12::kanMX6a; ubp10::natMX6a	Lab stock	74.79
55.34 with kanMX6:GAL1,10:GST:ubp10	Lab stock	60.62
55.34 with kanMX6:GAL1,10:ubp11	Lab stock	67.78
55.34 with kanMX6:GAL1,10:ubp12	Lab stock	69.01
55.34 with siz1::kanMX6	Lab stock	58.25
55.34 with ubp10:13MYC:hphMX4	Lab stock	59.57
55.34 with ubp10:13MYC:hphMX4; elg1::kanMX6	This study	77.40
55.34 with ubp12:13MYC:hphMX4	This study	71.01
55.34 with ubp12:13MYC:hphMX4; elg1::kanMX6	This study	77.45
55.34 with pol30:3FLAG:KanMX6	Lab stock	61.45
55.34 with pol30:3FLAG:KanMX6; ubp12:13MYC:HphMX4	Lab stock	70.73
55.34 with rev1:13MYC:HIS3	Lab stock	62.29.
55.34 with rev1:13MYC:HIS3 ubp10::kanMX6	This study	62.30
55.34 with rev1:13MYC:HIS3, ubp12::hphMX4, ubp10::natMX6	This study	71.72
55.34 with elg1::kanMX6	This study	77.38
55.34 with rev1:13MYC:HIS3; ubp10::NatMX6; ubp12::hphMX4; elg1::kanMX6	This study	80.18
55.34 with rev1:13MYC:HIS3; ubp10::NatMX6; ubp12::hphMX4; elg1::kanMX6;mms2::TRP1	This study	82.80
55.34 with elg1::kanMX6; rev1:13MYC:HIS3	This study	77.44
55.34 with rad52::natMX6	This study	79.68
55.34 with rad52::natMX6; ubp10::hphMX4	This study	79.71
55.34 with rad52::natMX6; ubp12::kanMX6	This study	79.73
55.34 with rad52::hphMX4; ubp12::kanMX6; ubp10::natMX6	This study	79.75
Mata ADE2 ura3-1 leu2-3,112 his3-11,15 trp1-1 can1-100 DDC2::MYC::TRP1	R. Bermejo	*RB292*
55.34 with ubp10^{C371S}:13MYC:hphMX4:URA3	This study	77.72
55.34 with ubp12^{C373S}:13MYC:hphMX4:URA3	This study	82.25
55.34 with sgs1::natMX6	This study	79.04
55.34 with ubp10::hphMX4; sgs1::natMX6	This study	79.08
55.34 with ubp12::kanMX6; sgs1::natMX6	This study	79.11
55.34 with ubp10::hphMX4; ubp12::kanMX6; sgs1::natMX6	This study	79.14
55.34 with ubp10::natMX6; elg1::kanMX6; rev1:13MYC:HIS3	This study	80.31
55.34 with ubp12::hphMX4; elg1::kanMX6; rev1:13MYC:HIS3	This study	80.32
55.34 with ubp10:13MYC:hphMX4; fen1:3FLAG:kanMX6	This study	81.13
55.34 with ubp10:13MYC:hphMX4; fen1:3FLAG:kanMX6	This study	81.14
55.34 with ubp12:13MYC:hphMX4; fen1:3FLAG:kanMX6	This study	81.16
55.34 with ubp10::hphMX4	This study	61.33
55.34 with rev1::kanMX6; rev3::TRP1; rad30::natMX6	This study	64.01
55.34 with ubp10::hphMX4; rev1::kanMX6; rev3::TRP1	This study	64.30

(*Continued on next page*)

Continued		
REAGENT or RESOURCE	SOURCE	IDENTIFIER
55.34 with ubp10::hphMX4; rev1::kanMX6; rev3::TRP1; rad30::natMX6	This study	64.31
55.34.08 with *pol30^{K164R}*	Lab stock	68.66
55.34.08 with *pol30^{K164R} ubp10::KanMX6*	Lab stock	68.51
55.34.08 with *pol30^{K164R} ubp12::hphMX4*	Lab stock	79.59
55.34.08 with *pol30^{K164R} ubp10::KanMX6; ubp12::hphMX4*	Lab stock	68.53
BY4741 *Mata his3Δ1 leu2Δ0 met15Δ0 ura3Δ0*	Lab stock	58.45
BY4741 58.45 with *ubp12:GAL1,10:HA:UBP12: HIS3*	This study	82.64
BY4741 58.45 with *rev3Δ::KanMX6*	Lab stock	61.81
BY4741 58.45 with *rev3Δ::KanMX6; ubp12:GAL1,10:HA:UBP12: HIS3*	This study	82.66
BY4741 58.45 with *mms2Δ::KanMX6*	Lab stock	69.11
BY4741 58.45 with *mms2Δ::KanMX6; ubp12:GAL1,10:HA:UBP12: HIS3*	This study	82.67
Schizosaccharomyces pombe h-; pcn1:3FLAG:KanMX6; ubp12:GFP-NES:NatMX4; ubp15:mRFP-NES:KanMX6; ubp16::HphMX4; ade6-M210; leu1-32; ura4D18	Lab stock	73.69
Oligonucleotides		
5′GTAACTTACACGGGGGCTAA3′ *ARS305*fw	This paper	N/A
5′ACTTTGATGAGGTCTCTAGC3′ *ARS305*rev	This paper	N/A
5′CACATTATTCGGCACAGTAGG3′ *ARS607*fw	This paper	N/A
5′GTGTCGCAGTCCATAGAAGG3′ *ARS607*rev	This paper	N/A
Software and Algorithms		
Tiling Array Suite Software (TAS)	Affymetrix	https://www.thermofisher.com/us/en/home/life-science/microarray-analysis.html

LEAD CONTACT AND MATERIALS AVAILABILITY

Further information and requests for resources and reagents should be directed to and will be fulfilled by the Lead Contact, Avelino Bueno (abn@usal.es). Yeast strains generated in this study are available on request without restriction.

EXPERIMENTAL MODEL AND SUBJECT DETAILS

Yeast Strains

All the budding yeast used in our studies originate from a *MATa* W303 *RAD5 bar1::LEU2* strain (Gallego-Sánchez et al., 2012) with the exception of the mutagenesis analysis made in BY4741 derivatives and are listed in the Key Resources Table. For the *in vitro* analysis of DUB activity, a fission yeast strain listed in the Key Resources Table was used as a source of ubiquitylated PCNA. Yeast strains were grown in YPA medium (1% yeast extract, 2% peptone, supplemented with 50 μg/ml adenine) containing 2% glucose. For block-and–release experiments, cells were grown in YPA with 2% glucose (except where indicated) at 25°C and synchronized with α-factor pheromone in G1 by adding 40 ng/ml (final concentration, 2.5 hours). Cells were then collected by centrifugation and released in fresh media in the absence or in the presence of HU or MMS (or other drugs as indicated). Overexpression experiments with cells grown in YPA medium with 2% raffinose at 25°C were conducted by adding to the medium 2.5% galactose (to induce) or 2% glucose (to repress) and further incubating with / without HU or MMS.

METHOD DETAILS

General Experimental Procedures and Flow Cytometry

General experimental procedures of yeast Molecular and Cellular Biology were used as described previously (Calzada et al., 2005; Cordón-Preciado et al., 2006; Sánchez et al., 1999). For flow cytometry, 10^7 cells were collected by centrifugation, washed once with water, and fixed in 70% ethanol and processed as described previously (Calzada et al., 2001; Sánchez et al., 1999). The DNA content

of individual cells was measured using a Becton Dickinson FACScan. Cells were prepared for flow cytometry, using a modification of the method of Hutter and Eipel (1979) (Calzada et al., 2001), by staining them with SYTOX Green (Molecular PROBES) following a technique previously described (Haase, 2004; Haase and Reed, 2002).

MMS and HU Sensitivity Assays

Exponentially growing or stationary cells were counted and serially diluted in YPA media. Ten-fold dilutions of equal numbers of cells were used. For each sample, 10 μL of each dilution were spotted onto YPAD (2% glucose) or YPAGal (2.5% galactose) plates (always supplemented with 50 μg/ml adenine), YPAD or YPAGal plates containing MMS (Sigma) or hydroxyurea (HU, FORMEDIUM), incubated at 25°C and scanned. MMS plates were always freshly made.

Tagging Yeast Proteins and Gene Deletion

To construct tagged alleles the single step PCR-based gene modification strategy by Longtine et al. (1998) was used. A similar strategy was used to generate specific gene deletions. The selection markers used were *KANMX6*, which allows selection with Geneticin, *HphMX4*, which allows selection with hygromicin or *NatMX6*, which allows selection with nourseothricin. We used also *URA3, TRP1* and *HIS3* markers (as indicated in Key Resources Table). The resulting genomic constructions were confirmed by PCR and sequencing. In the case of tagged alleles, the presence of tagged proteins was further confirmed by western blot. Since we used some C-terminally myc-tagged, FLAG- tagged and V5-tagged strains we carefully checked them all for growth rate, sensitivity to HU and MMS and found no differences with untagged controls.

Mutagenesis assays

Forward mutation analysis at the *CAN1* locus was performed essentially as described previously (Gallego-Sánchez et al., 2012). Cells of the strain background **BY4741** (Key Resources Table) were grown in rich medium (YPA Galactose) to log phase and MMS (0.005% v/v) was added to the half of each culture, which were further incubated until the saturation point was reached (60 hours). Then, cells were plated on solid medium, without arginine, containing 60 μg/ml canavanine (Sigma) and also in control YPAD plates (for reference). After 4 days, colonies were counted and the mutagenesis frequency (canavanine resistant cells versus total population/survivors) was calculated for each culture.

Immunoprecipitation, Western Blot Analysis and Antibodies

Protein Extract Preparation for Western Blot Analysis

TCA cell extracts were prepared and analyzed as described previously (Cordón-Preciado et al., 2006; Longhese et al., 1997). SDS-PAGE gels at 9%, 10%, and 12% were used for detection of Ubp10, Ubp12, and PCNA, respectively.

Protein Extract Preparation for Immunoprecipitations

Soluble protein extracts were prepared as described previously (Calzada et al., 2000; Gallego-Sánchez et al., 2012). Cells were collected, washed, and broken in HB2T buffer using glass beads. The HB2T buffer contained 60 mM β-glycerophosphate, 15 mM *p*-nitrophenylphosphate, 25 mM 4-morpholinepropanesulfonic acid (pH 7.2), 15 mM MgCl2, 15mM EGTA, 1 mM dithiothreitol, 0.1 mM sodium orthovanadate, 2% Triton X-100, 1 mM phenylmethylsulfonyl fluoride, and 20 mg/ml leupeptin and aprotinin. Glass beads were washed with 500 μL of HB2T, and supernatant was recovered. Protein concentrations were measured using the BCA assay kit (Pierce). After immunoprecipitation of PCNA or PCNA-FLAG, tagged proteins were detected by immunoblotting with specific monoclonal antibodies.

Western Blotting

Protein extracts and immunoprecipitates were electrophoresed using from 10 to 12% SDS-polyacrylamide gels. For western blots, 40-80 μg of total protein extracts from each sample were blotted onto nitrocellulose, and proteins were detected using a characterized anti-PCNA affinity-purified polyclonal antibody (1:1500; a generous gift from Dr. Paul Kaufmann). We also used the anti-FLAG monoclonal antibody (1:3000) the anti-V5(PK) monoclonal antibody (1:3000), or the anti-Myc monoclonal antibody (1:3000). Horseradish peroxidase-conjugated anti-rabbit, anti-goat, or anti-mouse antibodies (as required) and the ECL kit (Amersham Pharmacia Biotech) were used. The antibodies required for immunoblots were used at the indicated dilutions for western blot analysis.

In vitro deubiquitylation assays

PCNA-FLAG was efficiently immunoprecipitated from a *ubp12*-NES *ubp15*-NES *Δubp16 pcn1-FLAG S.pombe* strain (see Key Resources Table), synchronyzed in S-phase (2 hours in 20 mM HU). *S.pombe* PCNA is a reliable and abundant source of ubiquitylated PCNA lacking SUMO-PCNA (that would otherwise hamper our *in vitro* assay) (Álvarez et al., 2016). Ubp10-myc13 or Ubp12-myc13 were immunoprecipitated from asynchronous cultures of *S.cerevisiae* strains (we have found that budding yeast Ubp10 and Ubp12 are active all throughout the cell cycle). The immunoprecipitations were washed two times with lysis buffer and then twice with DUB buffer (60 mM HEPES at pH 7.6, 5 mM MgCl2, 4% glycerol). Beads were incubated overnight at 30°C. As negative controls, we used catalytically inactive Ubp10 and Ubp12 ($Ubp10^{CS}$ and $Ubp12^{CS}$ mutants) or (as well as active) Ubp10 and Ubp12 bound to ubiquitin vinyl sulfone (UbVS) DUB activity probe. This probe covalently captures active DUB enzymes and therefore acts as a potent and irreversible inhibitor of DUBs through the covalent modification of the active site, as previously described (Borodovsky et al., 2001). The UbVS probe was used as suggested by the manufacturer (Enzo Life Sciences).

ChIP-on-chip analysis

We adapted a ChIP-on-chip protocol for the analysis of PCNA-DUBs, myc-tagged Ubp10 and Ubp12, Mec1-associated protein Ddc2 and TLS polymerase ζ-associated Rev1 chromosomal binding (Bermejo et al., 2007; 2009b; Katou et al., 2003). *S. cerevisiae* oligonucleotide microarrays were provided by Affymetrix. The ChIP-on-chip method employed has been described in detail (Bermejo et al., 2009b). In brief, we disrupted 1.5 × 10^8 cells by FAstPreP FP120 (BIO101, Savant) using glass beads (G8772, Sigma-Aldrich) and anti-myc monoclonal antibodies clone 9E10 (M5546, Sigma-Aldrich) were used for ChIP. Control and chromatin-immunoprecipitated DNAs were purified and amplified using random priming PCR (WGA2 kit from Sigma-Aldrich): A total of 10 μg of amplified DNA was digested with DNase I to an average size of 100 bp and purified, and the fragments were end-labeled with biotin-N6-ddATP. Hybridization, washing, staining, and scanning were performed according to the manufacturer's instructions (Affymetrix).

ChIP-qPCR analysis

We also adapted a described protocol for the analysis of myc-tagged Ubp10, Ubp12, and TLS polymerase ζ-associated Rev1 *ARS305* or *ARS607* binding in *S. cerevisiae* cells in different genetic backgrounds and conditions as indicated (Frattini et al., 2017). In brief, after 30 min of crosslinking with 1% formaldehyde, cells were washed and homogenized. After cell breakage and sonication, extracts were clarified and soluble fractions were used for immunoprecipitation (3 to 4 hours at 4°C). Beads were washed as for CoIPs and chromatin was eluted in Elution Buffer (50 mM Tris-HCl ph 8.0, 10 mM EDTA, 1% SDS) incubating 10 min at 65°C. Samples were incubated overnight at 65°C in TE (+1% SDS) for de-crosslinking, treated with Proteinase K, DNA extracted by phenol/chlorophorm/isoamylalcohol pH 8.0 and treated with 0.3 μg/ml RNase A in TE. Finally, DNA was purified with QIAquick® PCR purification kit. 1-10 ng of immunoprecipitated or input DNA were amplified with iQ™ SYBR Green Supermix (BioRad) using a Real-Time PCR machine (BioRad IQ™ 5).

Two-dimensional DNA gels (2D-gel analysis)

DNA samples for neutral-neutral two-dimensional gel electrophoresis were prepared and analyzed as described previously (Calzada et al., 2005; Lopes et al., 2001). DNA was cut with the NcoI restriction enzyme and hybridized to probes spanning the *ARS305, ARS306* and *ARS1201* origins of DNA replication. For each origin of replication tested, the specific probe corresponds to the following coordinates (retrieved from SGD): *ARS305* (39073-40557, Chr III), *ARS306* (73001-73958, Chr III) and *ARS1200*-1 (458000-458985, Chr XII).

QUANTIFICATION AND STATISTICAL ANALYSIS

Mutagenesis assays

Mutagenesis frequency (measured by the appearance canavanine resistant colonies versus total population) was obtained by a fluctuation test as the median value of three independent cultures, with or without added MMS, for each indicated genotype. The given mutagenesis frequency is the mean and standard deviation of the median values from three biological replicates.

Statistical Analysis of Microarray data

Primary data analyses were carried out as described in the Supplemental Statistical Analysis document (section 1.5.a) in Bermejo et al. (2009a). In brief, clusters were identified using the Tilling Array Suite Software (TAS) as ranges within the chromosomes respecting the following conditions: estimated signal (IP/SUP binding ratio) positive in the whole range; change P value of the Wilcoxon signed rank test < 0.2 in the whole range, except for segments within the range shorter than 600 bp; size of the region of at least 600bp.

ChIP-qPCR analysis

All data in the bar graphs are presented as an average of $n \geq 3$ replicates ± standard deviation (SD), where n represents the number of biological replicates. The number of biological replicates are given in the figure legends when appropriate.

2D gel analysis of replication intermediates

Images were acquired using a Molecular Imager FX (BioRad) and different replication-associated DNA molecules were quantified using Quantity One 4.6 software (BioRad).

DATA AND CODE AVAILABILITY

Microarray data can be obtained from Gene Expression Omnibus database (GEO). The accession number for the ChIP-chip data reported in this database is GEO: GSE90157.